AD-A078 659 LOWELL UNIV MA F/G 4/2
THEORETICAL STUDY OF THREE DIMENSIONAL SLOPE AND VALLEY WIND SY--ETC(U)
NOV 79 W TANG , L N HOWARD , L N GUTMAN DAAG29-78-G-0012
UNCLASSIFIED ARO-12641.3-GS NL

END
DATE FILMED
1-80
DDC


1.0
1.1
1.25
1.4
1.6
1.8
2.0
2.2
2.5
2.8
3.2
3.6
4.0
4.5
5.0
5.6
6.3
MICROCOPY RESOLUTION TEST CHART
NATIONAL BUREAU OF STANDARDS-1963-A

UNIVERSITY OF LOWELL
LOWELL, MASSACHUSETTS 01854

LEVEL II

THEORETICAL STUDY OF THREE DIMENSIONAL SLOPE AND VALLEY WIND SYSTEMS

BY
Wen Tang
(Principal Investigator)
Louis N. Howard
Lev N. Gutman

Final Report Under Grant No. DAAG-29-78-G0012
For the period of 16 December 1977 - 30 July 1979
U.S. Army Research Office
Research Triangle Park, North Carolina

Unclassified

SECURITY CLASSIFICATION OF THIS PAGE (When Data Entered)

REPORT DOCUMENTATION PAGE

READ INSTRUCTIONS BEFORE COMPLETING FORM

1. REPORT NUMBER: 19 12641.3-GS (18 ARO)
2. GOVT ACCESSION NO.
3. RECIPIENT'S CATALOG NUMBER (9)
4. TITLE (and Subtitle): (6) Theoretical Study of Three Dimensional Slope and Valley Wind Systems.
5. TYPE OF REPORT & PERIOD COVERED: Final Report. 16 Dec 77 — 30 Jul 79
6. PERFORMING ORG. REPORT NUMBER
7. AUTHOR(s): (10) Wen Tung, Louis N. Howard, Lev N. Gutman
8. CONTRACT OR GRANT NUMBER(s): (15) DAAG29-78-G-0012
9. PERFORMING ORGANIZATION NAME AND ADDRESS: University of Lowell, Lowell, Massachusetts 01854 (12) 83
10. PROGRAM ELEMENT, PROJECT, TASK AREA & WORK UNIT NUMBERS
11. CONTROLLING OFFICE NAME AND ADDRESS: U. S. Army Research Office, P. O. Box 12211, Research Triangle Park, NC 27709
12. REPORT DATE: (11) Nov 79
13. NUMBER OF PAGES: 75
14. MONITORING AGENCY NAME & ADDRESS (if different from Controlling Office)
15. SECURITY CLASS. (of this report): Unclassified
15a. DECLASSIFICATION/DOWNGRADING SCHEDULE

LEVEL II

16. DISTRIBUTION STATEMENT (of this Report)

Approved for public release; distribution unlimited.

DDC RECEIVED DEC 20 1979 E

17. DISTRIBUTION STATEMENT (of the abstract entered in Block 20, if different from Report)

18. SUPPLEMENTARY NOTES

The view, opinions, and/or findings contained in this report are those of the author(s) and should not be construed as an official Department of the Army position, policy, or decision, unless so designated by other documentation.

19. KEY WORDS (Continue on reverse side if necessary and identify by block number)

mountain-valley terrain
mountain-valley wind system
wind systems
meso-scale flow
boundary layer problems
terrain

20. ABSTRACT (Continue on reverse side if necessary and identify by block number)

79 12 17 050

The meso-scale flow over and around a finite length of mountain ridge and typical mountain valley terrain is studied. The present study is different from earlier analytical lee wave studies in that the solution is truly three-dimensional for more realistic topography. A simple model is developed and is attacked by multiple-scaling approach. The solutions are not only valid for large distances in the downwind direction, but are also good for the near regions. The phase lines of the vertical velocity on a horizontal plane at a

DD FORM 1 JAN 73 1473 EDITION OF 1 NOV 65 IS OBSOLETE

Unclassified

S/C 392 784

20. ABSTRACT CONTINUED

given height have shape of hyperbolas and are concave toward downwind side in accord with observations. The wind component parallel to the mountain ridge is found to be diffluent on the windward slope side, continuing to be so after crossing over the ridge in the lowest layer, and to become confluent at some distance downwind from the ridge. The intensity of the lee wave over a valley relates to the separation between the two ridges and the stability. Just above the valley floor, wind parallel to valley axis is in the down valley direction and thus raises the height of the maximum down-valley wind much higher than that of maximum 'slope wind' above the valley sides during the night. The computation also shows the increase of its intensity and height of occurance with down-valley distance. In the farther downwind direction of the lee, the maximum confluent flow along the ridge is found at a much lower level and is stronger. The intensity and the position of the maximum wind parallel to the valley or the mountain ridges is closely related to the downslope motion of the lee wave.

PREFACE

The thermally induced mountain-valley wind system and its interaction with the large or meso-scale flow has always interested meteorologists and other professionals directly involved with the development of the wind system. Various analytical and numerical studies have been pursued and have yielded some interesting results. Yet many phenomena in the local wind system have not really been explored and explained satisfactorily. For example, the problem concerning the speed and height of the maximum wind or local jet along the valley axis remains unclear. Whether they result from direct influence of the basic background flow or just the pure local thermal boundary larger effect or from interaction of both requires a further understanding of some basic problems of flow over and around typical mountain-valley terrain and the development of a better method to solve the complicated problem of sophisticated model of boundary layer dynamics.

In the first part, we developed a model to study the flow over and around more realistic three-dimensional mountain-valley terrain and utilized a multiple scaling approach to obtain truly three-dimensional flow solutions for the near region, as well as for a large distance from the ridges in the lee. The theoretical findings from the lee-wave over the lee-slope are in accord with some observations and other studies. This investigation is different from many other previous studies in that the flow around the ridge and along the valley has enabled us to visualize how interaction between the meso-scale flow and the valley wind system in the lower layer takes place and to understand better the wind structure under such circumstances. The solution for the wind component in a direction parallel to the ridges or in the valley direction explains some puzzling and interesting valley-wind phenomena.

For the second part, studies of boundary layer problems are presented. The parameterization of the surface layer and active soil layer with moisture and precipitation contributions is made for meso-scale dynamics. It can be used for mountain-valley circulation as long as the slope of the terrain is not exceedingly large and some other basic conditions are met. With this parameterization the boundary conditions for the governing prediction equations of mountain-valley wind problems in numerical models can be appropriately constructed. Applying these improved boundary conditions will facilitate the solution of the numerical model of the boundary layer and over meso- or large-scale circulation problems and can also produce more realistic results.

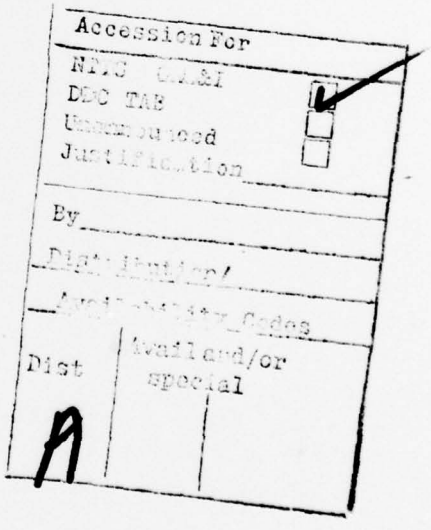

THEORETICAL STUDY
OF
THREE-DIMENSIONAL SLOPE
AND
VALLEY WIND SYSTEMS

PART I. THREE-DIMENSIONAL LEE WAVE AND ITS EFFECT ON THE SLOPE AND VALLEY WIND SYSTEMS

Wen Tang
University of Lowell
Lowell, Massachusetts 01854

Louis N. Howard
Massachusetts Institute of Technology
Cambridge, Massachusetts 02139

TABLE OF CONTENTS

LIST OF FIGURES

ABSTRACT

The meso-scale flow over and around a finite length of mountain ridge and typical mountain valley terrain is studied. The present study is different from earlier analytical lee wave studies in that the solution is truly three-dimensional for more realistic topography. A simple model is developed and is attacked by multiple-scaling approach. The solutions are not only valid for large distances in the downwind direction, but are also good for the near regions. The phase lines of the vertical velocity on a horizontal plane at a given height have shape of hyperbolas and are concave toward downwind side in accord with observations. The wind component parallel to the mountain ridge is found to be diffluent on the windward slope side, continuing to be so after crossing over the ridge in the lowest layer, and to become confluent at some distance downwind from the ridge. The intensity of the lee wave over a valley relates to the separation between the two ridges and the stability. Just above the valley floor, wind parallel to valley axis is in the down valley direction and thus raises the height of the maximum down-valley wind much higher than that of maximum 'slope wind' above the valley sides during the night. The computation also shows the increase of its intensity and height of occurance with down-valley distance. In the farther downwind direction of the lee, the maximum confluent flow along the ridge is found at a much lower level and is stronger. The intensity and the position of the maximum wind parallel to the valley or the mountain ridges is closely related to the downslope motion of the lee wave.

I. INTRODUCTION

Previous theoretical studies of lee waves are numerous. Most attention has been focussed on two-dimensional lee wave-waves behind an infinitely long ridge. Earlier works on three-dimensional lee waves are essentially limited to simple topography.

Scorer and Wilkinson (1956) studied waves in the lee of both isolated circular and oval-shaped hills in a two-layer model atmosphere. In each layer, the "Brunt-Väisälä frequency over mean wind speed" is assumed constant. They found that the wave disturbance is essentially confined to a wedge (for example, with wake angle of 24^{o} in one case) and has the form of a shipwave. Assuming an isothermal atmosphere with uniform wind velocity, and ground surface as a stepped plateau of finite width, Wurtele (1957) was able to show the wave nodal lines in a horizontal plane are rectangular hyperbolas concave downwind, in qualitative agreement with clouds observed in the lee of Mt. Fuji and laboratory experiments by Abe (1941). Although he cannot use his one layer model to show the shipwave type disturbance, Wurtele pointed out, in a later paper concering cloud photographies for the lee of San Nicolas Island (Endinger and Wurtele, 1972) that when a strong temperature inversion occurs, a classical shipwave disturbance will develop instead of a cresent-shaped pattern.

Palm (1958) considered the case when the basic wind increases linearly with height in the troposhere and stays constant in the stratosphere, while the stabilities are constant in both layers. For a circular hill, Palm obtained a solution for the vertical velocity and found that the lee waves are also confined to a wedge in the downwind direction, but only for sections at a relatively large distance from the hill. In extending his method of study of two-dimensional lee waves, Onishi (1960) sought a solution for three-dimensional lee waves due to a circular hill in the atmosphere with both zero and constant wind shear in the vertical direction. As done by Scorer and Wilkinson, Wurtele, and Palm, Onishi also applied the method of stationary phase to obtain the solution. For the case of constant shear, he managed to increase the wake angle from a small wedge to a value beyond which no stationary point can be obtained.

In consequence, there is no lee wave found outside this maximum wake angle. As for the case where there is constant wind and strong stability, the disturbance is confined to a strip. Crapper investigated lee wave problems for a circular mountain first and then a mountain with elliptical contours (1962). For the latter study, constant wind shear together with both thermal stability conditions constant and an exponentially decreasing with height were considered. Under the constant stability condition, he found that the waves are confined to a strip for the case of no shear, whereas the waves are confined to a wedge resembling shipwaves for the case with a large constant shear. For the case without wind shear, the amplitude of the waves in the central plane in the downwind direction of an elliptical mountain is greater than that of an infinite ridge. The magnitude of the vertical disturbance decays in a form inversely proportional to three halves (3/2) power of the downwind distance. The results appear to be controversial.

Evaluation of integrals by numerical methods or the use of numerical models for studies of three-dimensional lee wave problems has increased recently. A three-dimensional lee wave for an isolated nearly circular hill was studied with the perturbation method but integrated numerically in both two- and three-layer models by Sawyer (1962). In his model, the horizontal wind velocity can change with height in direction, as well as in speed. The computed vertical velocities due to the lee waves have a series of bow-shaped patterns concave downwind and which are also confined to a wedge similar to those obtained by others The maximum magnitude occurs just off the peak of the hill and decreases gradually away from the hill. By being aware that the lee wave disturbance is essentially confined to a wedge and applying a transformation to an oblique co-ordinate system, Pekelis (1966) developed an algorithm for solving the non-linear three-dimensional lee wave problem. Computations show that the height of an obstacle definitely influences the shape of the pattern of vertical velocity in the non-linear model. For high steep mountains where the non-linear process is important, the pattern differs strikingly from that of relatively low obstacles in that the nodal lines of the vertical velocity are convex downwind, almost opposite to the shipwave or bow-shape wave.

Vergeiner (1975, 1976) developed a three-dimensional, time dependent, linearized numberical model to study Foehn wind and lee wave flow. For the circular hill case he produced a more or less similar kind of vertical velocity pattern as obtained by others except that some computing noises are involved. He also applied the model to study the flow over the smoothed topography of a part of the Tyrol Province of Austria and selected soundings yielded interesting results. Some topographically produced features under the interaction between orographically forced and free waves are still recognizable in the computed wind field. The computed results are generally, also, in agreement with other theoretical and observational evidence.

Considering both cross-wind and vertical shear, Blumen et al.,(1975) attacked the three-dimensional lee wave behind a nearly circular mountain. The vertical velocity field is obtained in Fourier integeral and evaluated numerically. One of the interesting results is that when the constant basis wind velocity is 23 $msec^{-1}$, the maximum upward vertical velocity is about 2.5 cm sec^{-1} at height 2 km and distance 2 km downwind from the center of the mountain which has a peak height of about 570 m. This vertical velocity is a much lower value than the one usually obtained by other authors.

Most recently, Gjevik et al (1978) applied a kinematic method developed by Whitham to investigate the wake angle of shipwave type patterns of the phase lines of the vertical velocity. The computed wave patterns under various conditions are qualitatively in agreement with some satellite cloud photographs.

The purpose of the present investigation is to study the three-dimensional lee wave above the flow over and around a ridge of finite length and above a typical mountain-valley terrain, and its effects on the mountain-valley wind system. The problem is studied based on a simple linearized model and is solved with the multiple scaling approach so that representative solutions can be obtained for both the near region and the far region of the mountain terrain in the downwind direction. From the theoretical study, the basic structure of the velocity field in the lee of the finite ridge and above a typical valley is obtained when the thermal boundary layer influence is minimum. Because of our

interest in effects on valley winds, we direct more attention to the near field than has often been the case in the lee wave studies. In Section 2, a general description is presented. The development of the solutions based on the multiple-scaling method and the numerical results of the solutions are given in Sections 3 and 4. A brief conclusion and recommendations can be found in Section 5.

II. THE MODEL

Since our main interest is to explore the consequences of mountain waves for valley winds, we simplify as much as possible the mountain wave aspect by considering a time-independent Boussinesq, incompressible, stratified inviscid fluid, and linearize about a basic state with velocity $U(Z)>0$ in the x-direction, and thermal stratification $T_o(Z)$. Thus, our basic equations for the perturbation velocity $\underline{u}$ and temperature θ are:

$$U\underline{u}_x + wU'\underline{i} + \frac{1}{\rho_o}\nabla p - \alpha g\theta\underline{\kappa} = 0, \quad \nabla\cdot\underline{u} = 0, \text{ and } U\theta_x + wT_o' = 0.$$

(α is the thermal expansion coefficient.) Eliminating all the dependent variables except w amont these equations one obtains

$$\nabla^2 w_{xx} - \frac{U''}{U} w_{xx} + \frac{N^2}{U^2}\nabla_1^2 w = 0 \tag{1}$$

where ∇_1^2 is the horizontal Laplace operator and $N^2 = \alpha g T_o'$ is the square of the Brunt-Väisälä frequency.

We take this equation on $0\leq Z\leq \pi H$ with the boundary conditions

$$w = U(o)\frac{\partial h}{\partial x} \quad \text{on } Z = 0 \tag{2a}$$

$$w = 0 \qquad \text{on } Z = \pi H \tag{2b}$$

The function h in (2a) represents, on the linear theory, the height of the mountain as a function of the horizontal coordinates. We are going to assume that the characteristic scale of variation of h, in its dependence on x, is of the same order as the depth πH of the layer. However, its characteristic scale of variation in y is taken to be larger by a factor of ε^{-1}, where ε is a small parameter. It is this aspect ratio parameter ε which we shall exploit in solving the problem; the small parameter implicitly already used in making the linearization may be taken to be the ratio h_o/H, where h_o is, say, the maximum height of the mountain.

We assume h tends to zero (with sufficient rapidity for mathematical needs) as x or $y \to \pm\infty$. We shall give explicit calculations for the example:

$$h = h_o \exp\left[-K|x/H| - (\varepsilon y/H)^2\right] \tag{3}$$

(In place of (2b) one could also consider an unbounded layer, H then being an appropriate scale height for the velocity and stratification profiles; if the latter are such as to admit wave propagation at large Z, the condition $w \to o$ would then be replaced by an outgoing wave condition.)

We introduce dimensionless position coordinates temporarily distinguished by overbars, by

$$x = \bar{x}H, \quad y = \bar{y}H, \quad Z = \bar{z}H$$

and also set $\varepsilon\bar{y} = Y$. We set

$$h = h_o\bar{h}(\bar{x},Y), \quad U = U(o)\bar{U}(\bar{z}), \quad N^2U^{-2} = H^{-2}J(\bar{z})$$

and for the dependent variables take:

$$u = U(o)h_oH^{-1}\bar{u}, \quad v = \varepsilon U(o)h_oH^{-1}\bar{v},$$

$$w = U(o)h_oH^{-1}\bar{w}, \quad \theta = U(o)^2h_o(\alpha gH^2)^{-1}\bar{\theta}$$

$$p = \rho_o U(o)^2 h_o H^{-1}\bar{p}$$

Then the basic equations become, on dropping the overbars;

$$Uu_x + U'w + p_x = 0 \tag{4a}$$

$$Vv_x + p_Y = 0 \tag{4b}$$

$$Uw_x - \theta + p_z = 0 \tag{4c}$$

$$\theta_x + UJw = 0 \tag{4d}$$

$$u_x + \varepsilon^2 v_Y + w_z = 0 \tag{4e}$$

and equation (1) for w alone becomes

$$\left[\frac{\partial^2}{\partial x^2} + \frac{\partial^2}{\partial z^2} - \frac{U''}{U} + J\right]\frac{\partial^2 w}{\partial x^2} + \varepsilon^2\left[\frac{\partial^2}{\partial x^2} + J\right]\frac{\partial^2 w}{\partial y^2} = 0 \tag{5}$$

The dimensionless form of the boundary conditions (2) is

$$w = \frac{\partial h}{\partial x} \qquad \text{on } z = 0 \tag{6a}$$

$$w = 0 \qquad \text{on } z = \pi \tag{6b}$$

We have used U(o) as the characteristic scale for the velocity profile; this would of course not be appropriate if U(o) = 0; by in such a case neither would be the linearization. In the calculations using (3), which in dimensionless form is

$$h = \exp\left[-K|x|-Y^2\right] \tag{7}$$

we shall also take U and J to be constants.

In addition to these boundary conditions, we have the conditions of no upstream influence, meaning that w (and the other perturbation quantities as well) should tend to zero for $x \to -\infty$, and downstream boundedness, meaning that they should bounded for $x \to +\infty$. We also assume that they tend to zero as $Y \to \pm\infty$ for any fixed x. Actually, we are considering a family of problems parameterized by ε, and we shall require these conditions expressed in the above dimensionless form, to hold uniformly in ε, as $\varepsilon \to o^+$. We shall also be concerned to find a representation of the solutions which is uniformly valid in as large a domain as possible as $\varepsilon \to o$. If the problem is attacked as a perturbation problem in ε in the most straightforward way, one does not, in fact, get a representation uniformly valid for large x; in order to obtain a relatively simple and useful description of the flow a somewhat different approach is needed. We shall see that there are, in fact, three different scales in x, $x = O(1)$, $O(\varepsilon^{-1})$, and $O(\varepsilon^{-2})$, which are important in this description; this will be clarified by consideration of the specific example (7), to which we now proceed.

III THE SOLUTIONS

We now take U and J to be constants, so U = 1; we assume J>0 (static stability). Let $w^{(n)}(x,Y)$ to be the Fourier sine coefficients of w on $0 \le Z \le \pi$:

$$w^{(n)} = \frac{2}{\pi}\int_0^{\pi} \sin nz\, w\, dz$$

We shall represent w by its sine series, but since w does not vanish on Z = 0, the terms of this series will only tend to zero like 1/n. Thus the series will not be directly useful for computation; we shall consider later how it can be improved. More important is the fact that formal term by term differentiation of the series does not give, for example, the correct sine series of $\frac{\partial^2 w}{\partial z^2}$. Thus, the sine series should not simply be substituted into eq (5). However, the consequences of (5) for the $w^{(n)}$ are readily obtained by multiplying it by $(2/\pi)$ sin nz and integrating from 0 to π. On integrating the term involving $\partial^2 w/\partial z^2$ twice by parts, using equations (6) one obtains:

$$\left(\frac{\partial^2}{\partial x^2} - n^2 + J\right)\frac{\partial^2 w^{(n)}}{\partial x^2} + \varepsilon^2\left(\frac{\partial^2}{\partial x^2} + J\right)\frac{\partial^2 w^{(n)}}{\partial y^2} = -\frac{2n}{\pi}\frac{\partial^3 h}{\partial x^3} \qquad (8)$$

Now take the Fourier transform in Y of this equation, setting $\bar{w}^{(n)} = \int_{-\infty}^{\infty} e^{ikY} w^{(n)} dy$,

this gives:

$$\left(\frac{\partial^2}{\partial x^2} - n^2 + J\right)\frac{\partial^2 \bar{w}^{(n)}}{\partial x^2} - \varepsilon^2 k^2\left(\frac{\partial^2}{\partial x^2} + J\right)\bar{w}^{(n)} = -\frac{2n}{\pi}\frac{\partial^3 \bar{h}}{\partial x^3} \qquad (9)$$

For h given by (7), we have

$$\frac{\partial^3 \bar{h}}{\partial x^3} = -K^3\sqrt{\pi}e^{-K|x|-k^2/4}\operatorname{sgn}(x). \qquad (10)$$

Because of the discontinuity in $\frac{\partial h}{\partial x}$ at x = 0 we shall consider separately the cases of positive and negative x, applying appropriate matching conditions at the origin. To obtain these conditions, we look also at the other components of the flow, representing u, v and p by cosine series of the form $u = \frac{1}{2}u^{(o)} + \sum_{1}^{\infty} u^{(n)} \cos nz, \left(u^{(n)} = \frac{2}{\pi} \int_{o}^{\pi} u \cos nz \, dz \right)$, and θ by a sine series as in the case of w. Taking also the Fourier transform with respect to Y, equations (4) (for the present example) then give:

$$\bar{u}^{(n)}_x + \bar{p}^{(n)}_x = 0 \qquad (n \geq o) \qquad (11a)$$

$$\bar{v}^{(n)}_x - ik\bar{p}^{(n)} = 0 \qquad (n \geq o) \qquad (11b)$$

$$\bar{w}^{(n)}_x - \bar{\theta}^{(n)} - n\bar{p}^{(n)} = 0 \qquad (n \geq 1) \qquad (11c)$$

$$\bar{\theta}^{(n)} + J\bar{w}^{(n)} = 0 \qquad (n \geq 1) \qquad (11d)$$

$$\bar{u}^{(n)}_x - ik\epsilon^2\bar{v}^{(n)} + n\bar{w}^{(n)} = \frac{2}{\pi}\bar{h}_x \qquad (n \geq o) \qquad (11e)$$

At x=o we want u, v, w, θ and p to be continuous. Writing $\left[f \right] = f(o+) - f(0-)$ we thus get:

$$\left[\bar{w}^{(n)} \right] = 0 \qquad (12a)$$

$$\left[\bar{w}^{(n)}_x \right] = 0 \qquad (12b)$$

using (11c). Differentiating (11c) and using the other equations shows that

$$\left[\bar{w}^{(n)}_{xx} \right] = \left[\bar{\theta}^{(n)}_x \right] + n \left[\bar{p}^{(n)}_x \right] = -J \left[\bar{w}^{(n)} \right] - n \left[\bar{u}^{(n)}_x \right] = -\frac{2n}{\pi} \left[\bar{h}_x \right] .$$

Similarly $\left[\bar{w}^{(n)}_{xxx}\right] = \left[\bar{\theta}^{(n)}_{xx} + n\bar{p}^{(n)}_{xx}\right] = -J\left[w^{(n)}_{x}\right]$

$$-n\left[\bar{u}^{(n)}_{xx}\right] = -ikn\varepsilon^2\left[\bar{v}^{(n)}_{x}\right] + n^2\left[w^{(n)}_{x}\right] - \frac{2n}{\pi}\left[\bar{h}_{xx}\right]$$

$$= -\frac{2n}{\pi}\left[\bar{h}_{xx}\right] .$$

Since $\bar{h} = \sqrt{\pi}e^{-k|x|-k^2/4}$, we thus get

$$\left[\bar{w}^{(n)}_{xx}\right] = 4n\pi^{-1/2}Ke^{-k^2/4} \tag{12c}$$

and

$$\left[\bar{w}^{(n)}_{xxx}\right] = 0 \tag{12d}$$

Now, using (10) we can write down at once a particular solution (for $x \neq 0$) of (9):

$$P = P_o e^{-K|x|}\,\mathrm{sgn}x = \frac{2n\pi^{-1/2}Ke^{-k^2/4}}{(K^2-n^2+J) - \varepsilon^2k^2(1+J/K^2)}\, e^{-K|x|}\,\mathrm{sgn}x, \tag{13}$$

P_o being defined thereby. Note that (12c) can then be written as

$$\left[\bar{w}^{(n)}_{xx}\right] = 2P_o\left[K^2-n^2+J - \varepsilon^2k^2(1+J/K^2)\right] \tag{12c}$$

P satisfies (9) and tends to zero at $\pm\infty$, but is not continuous at x=0. The solutions of the homogeneous form of (9) are combinations of exponentials $e^{\pm\lambda x}$ where λ^2 is a root of the quadratic

$$\lambda^2(\lambda^2-n^2+J) - \varepsilon^2k^2(\lambda^2+J) = 0$$

When ε^2 is small, one of the roots is near 0 and the other near n^2-J; since their product is $-\varepsilon^2k^2J$, they are always real and of opposite sign.

Let the positive root be called ℓ^2 and the negative one $-L^2$:

$$\ell^2 = \frac{1}{2}\left[n^2-J+\epsilon^2k^2+\sqrt{(n^2-J+\epsilon^2k^2)^2+4\epsilon^2k^2J}\right] \tag{14a}$$

$$L^2 = \frac{1}{2}\left[-n^2+J-\epsilon^2k^2+\sqrt{(n^2-J+\epsilon^2k^2)^2+4\epsilon^2k^2J}\right]$$

(Which of these is near 0 and which near n^2-J depends on the sign of $n^2-J+\epsilon^2k^2$.) Then the solutions of (9) which tend to zero for $x\to-\infty$ and are bounded for $x\to+\infty$ are of the form:

$$\bar{w}^{(n)} = P + Ae^{\ell x} \qquad \text{(XLO)} \tag{15a}$$

$$= P + Be^{-\ell x} + C\cos Lx + D\sin Lx \qquad (x>o) \tag{15b}$$

The conditions (12) then give the following equations for A, B, C, and D:

$$\begin{aligned}
-A + B + C &= -2P_o \\
-\ell A - \ell B + LD &= 0 \\
-\ell^2 A + \ell^2 B - L^2 C &= 2P_o\left[-n^2+J-\epsilon^2k^2(1+J/K^2)\right] \\
-\ell^3 A - \ell^3 B - L^3 D &= 0
\end{aligned}$$

The solution of these equations is

$$\left.\begin{aligned}
A = -B &= P_o\left[\ell^2+\epsilon^2k^2J/K^2\right]/(L^2+\ell^2) \\
C &= 2P_o\left[-L^2+\epsilon^2k^2J/K^2\right]/(L^2+\ell^2) \\
D &= 0
\end{aligned}\right\} \tag{16}$$

In principle, this gives the solution to our problem, but because of the somewhat complicated way that L^2 and ℓ^2 depend on k^2 it does not seem to be possible to invert the Fourier transform in terms of simple formulas.

However, we can now use the small parameter ε to obtain more tractable approximations. We have, first,

$$L^2+\ell^2=\left[(n^2-J+\varepsilon^2k^2)^2+4\varepsilon^2k^2J\right]^{1/2}=|n^2-J|+\varepsilon^2k^2(n^2+J)/|n^2-J|+0(\varepsilon^4),$$

and so

$$\ell^2=\frac{1}{2}\left[n^2-J+|n^2-J|\right]+\frac{\varepsilon^2k^2}{2}\left[\frac{(n^2-J|+n^2+J}{|n^2-J|}\right]+0(\varepsilon^4) \tag{17a}$$

$$L^2=\frac{1}{2}\left[J-n^2+|n^2-J|\right]+\frac{\varepsilon^2k^2}{2}\left[\frac{n^2+J-|n^2-J|}{|n^2-J|}\right]+0(\varepsilon^4) \tag{17b}$$

Also,

$$P_o=\frac{2n\pi^{-\frac{1}{2}}Ke^{-k^2/4}}{K^2-n^2+J}\left[1+\varepsilon^2k^2\,\frac{1+J/K^2}{K^2-n^2+J}+0(\varepsilon^4)\right] \tag{18}$$

Let us write n_* for the integral part of $J^{\frac{1}{2}}$, supposing (as has already implicitly been done in writing down (17) that J is not a square integer. Then equations (17) become

$$\left.\begin{aligned}\ell^2&=\varepsilon^2k^2J/(J-n^2)+0(\varepsilon^4)\\ L^2&=J-n^2+\varepsilon^2k^2n^2/(J-n^2)+0(\varepsilon^4)\end{aligned}\right\}\quad(n\le n^*) \tag{19}$$

or

$$\left.\begin{aligned}\ell^2&=n^2-J+\varepsilon^2k^2n^2/(n^2-J)+0(\varepsilon^4)\\ L^2&=\varepsilon^2k^2J/(n^2-J)+0(\varepsilon^4)\end{aligned}\right\}\quad(n>n^*) \tag{20}$$

Using these and (18) in (16) we find, setting

$$P_o^o=2n\pi^{-\frac{1}{2}}Ke^{-k^2/4}/(K^2-n^2+J),$$

$$\left.\begin{aligned}A=-B&=P_o^o\varepsilon^2k^2J\,\frac{K^2-n^2+J}{K^2(J-n^2)^2}+0(\varepsilon^4)\\ C&=-2P_o^o\left(1+\frac{\varepsilon^2k^2(n^4-JK^2-J^2)}{(J-n^2)^2(K^2-n^2+J)}+0(\varepsilon^4)\right)\end{aligned}\right\}\quad(n\le n_*) \tag{21}$$

or

$$A = -B = P_o^o\left(1+\frac{\varepsilon^2k^2(n^4-JK^2-J^2)}{(n^2-J)^2(K^2-n^2+J)} + O(\varepsilon^4)\right)$$

$$C = -2P_o^o\ \varepsilon^2k^2J\cdot\frac{K^2-n^2+J}{K^2(n^2-J)^2}+O(\varepsilon^4) \qquad (n>n_*) \qquad (22)$$

In order to obtain a representation of the solution which is uniformly valid over as large a range of x as possible one should not, however, simply expand the functions $e^{-\ell|x|}$ and cosLx in powers of ε. It is better to follow the general idea of multiple scaling, introducing new variables $\xi = \varepsilon x$ and $X = \varepsilon^2 x$ (and possibly $X_3 = \varepsilon^3 x$ etc., though we shall not use these) so as to obtain a representation of the form $w = w_0(x,\xi,X,Y,z)+\varepsilon^2 w_2 + \ldots$ in which the second term is in fact of order ε^2 compared with the first even when x is as large as ε^{-2}. Thus in using the above approximations in (15) we write in the "wave case", $n\le n_*$:

$$\bar{w}^{(n)} = P_o^o\left[1+\varepsilon^2k^2\frac{1+J/K^2}{K^2-n^2+J}+\ldots\right]e^{-K|x|}\operatorname{sgn}x$$

$$-P_o^o\varepsilon^2k^2J\frac{K^2-n^2+J}{K^2(J-n^2)^2}\ e^{-|k||\xi|(J/(J-n^2))^{1/2}}\ \operatorname{sgn}x+\ldots$$

$$-P_o^o(1+\operatorname{sgn}x)\left(1+\varepsilon^2k^2\frac{n^4-JK^2-J^2}{(J-n^2)^2(K^2-n^2+J)}+\ldots\right)\cos\left(\sqrt{J-n^2}\,x\right.$$

$$\left.+\frac{k^2n^2}{2(J-n^2)^{3/2}}X\right), \qquad (n\le n_*) \qquad (23)$$

and in the "evanescent case", $n>n_*$:

$$\bar{w}^{(n)} + P_o^o\left[1+\varepsilon^2k^2\frac{1+J/K^2}{K^2-n^2+J}+\ldots\right]e^{-K|x|}\operatorname{sgn}x$$

$$-\operatorname{sgn}xP_o^o\left[1+\varepsilon^2k^2\frac{n^4-JK^2-J^2}{(n^2-J)^2(K^2-n^2+J)}+\ldots\right]e^{-\left(\sqrt{n^2-J}\,|x|+\frac{n^2k^2|X|}{2(n^2-J)^{3/2}}\right)}$$

$$-P_o^o\ (1+\operatorname{sgn}x)\varepsilon^2k^2J\ \frac{K^2-n^2+J}{K^2(n^2-J)^2}\ \cos k\xi(J/(n^2-J))^{1/2} \qquad (n>n_*) \qquad (24)$$

The other components of the flow, for $n \geq 1$, can also be obtained by using equations (11); the results are:

$$\bar{u}^{(n)} = \left\{ \frac{1}{n} \frac{K^2+J}{K} P_o e^{-K|x|} - \frac{\ell^2+J}{\ell} A e^{-\ell|x|} - \frac{1+\mathrm{sgn}x}{2} C \frac{J-L^2}{L} \sin Lx \right\} , \tag{25a}$$

$$\bar{v}^{(n)} = \frac{ik}{n} \left\{ \frac{K^2+J}{K^2} P_o e^{-K|x|}\mathrm{sgn}x - \frac{\ell^2+J}{\ell^2} A e^{-\ell|x|}\mathrm{sgn}x - \frac{1+\mathrm{sgn}x}{2} C \frac{J-L^2}{L^2} \cos Lx \right\} , \tag{25b}$$

$$\bar{p}^{(n)} = -\frac{1}{n} \left\{ \frac{K^2+J}{K} P_o e^{-K|x|} - \frac{\ell^2+J}{\ell} A e^{-\ell|x|} - \frac{1+\mathrm{sgn}x}{2} C \frac{J-L^2}{L} \sin Lx \right\} , \tag{25c}$$

$$\bar{\theta}^{(n)} = J \left\{ \frac{1}{K} P_o e^{-K|x|} - \frac{A}{\ell} e^{-\ell|x|} - \frac{1+\mathrm{sgn}x}{2} \frac{C}{L} \sin Lx \right\} . \tag{25d}$$

$\bar{u}^{(o)}$, $\bar{v}^{(o)}$ and $\bar{p}^{o}$ are not determined by w, but are obtained by solving the n=o cases of (11a, b, e) namely:

$$\bar{u}^{(o)}_x + \bar{p}^{(o)}_x = 0 \tag{26a}$$

$$\bar{v}^{(o)}_x - ik\bar{p}^{(o)} = 0 \tag{26b}$$

$$\bar{u}^{(o)}_x - ik\epsilon^2\bar{v}^{(o)} = \frac{2}{\pi} \bar{h}_x = -2\pi^{\frac{1}{2}} K e^{-K|x|-k^2/4}\mathrm{sgn}x \tag{26c}$$

These imply

$$\bar{u}^{(o)}_{xx} - k^2\epsilon^2\bar{u}^{(o)} = 2\pi^{-\frac{1}{2}} K^2 e^{-K|x|-k^2/4} ,$$

so

$$\bar{u}^{(o)} = 2\pi^{-\frac{1}{2}} \frac{K^2}{K^2-k^2\epsilon^2} e^{-K|x|-k^2/4} + Ee^{-|k|\epsilon|x|} . \tag{27}$$

(26c) shows that for continuity of $\bar{v}^{(o)}$ at $x=o$ we have $\left[\bar{u}_x^{-o}\right] = -4\pi^{-\frac{1}{2}}Ke^{-k^2/4}$; since (27) gives $\left[\bar{u}_x^{-o}\right] = -4\pi^{-\frac{1}{2}}K^3e^{-k^2/4}/(K^2-k^2\varepsilon^2) - 2\varepsilon|k|E$ we get

$$E = \frac{2\pi^{-\frac{1}{2}}Ke^{-k^2/4}}{\varepsilon|k|}\left(1 - \frac{K^2}{K^2-k^2\varepsilon^2}\right) = \frac{-2\pi^{-\frac{1}{2}}K|k|\varepsilon}{K^2-k^2\varepsilon^2}\, e^{-k^2/4}$$

Thus

$$\bar{u}^{(o)} = \frac{2\pi^{-\frac{1}{2}}K^2e^{-k^2/4}}{K^2-k^2\varepsilon^2}\left(e^{-K|x|} - \frac{\varepsilon|k|}{K}\, e^{-\varepsilon|k||x|}\right) \tag{28a}$$

$$\bar{v}^{(o)} = i\frac{2\pi^{-\frac{1}{2}}kKe^{-k^2/4}}{K^2-k^2\varepsilon^2}\left(e^{-K|x|} - e^{-\varepsilon|k||x|}\right)\,\mathrm{sgn}x \tag{28b}$$

$$\bar{p}^{(o)} = -\bar{u}^{(o)} \quad . \tag{28c}$$

For small ε, the factor $(K^2-k^2\varepsilon^2)^{-1}$ in (28) may be replaced by $K^{-2}(1+k^2\varepsilon^2/K^2\ldots)$ in the same manner as in obtaining (23) and (24). It should perhaps be remarked that since these expansions in powers of ε^2 are not uniform in k^2 - in fact they should only be used for ε^2k^2/K^2 small - we should not, strictly speaking, use them in evaluating the inverse Fourier transforms. However, because of the factor $e^{-k^2/4}$ we may cut off the inverse Fourier integral at a finite value of k, for instance $k = K\varepsilon^{-\frac{1}{2}}$, thereby incurring only a transcendatally small error. In the truncated integral, the expansions are legitimate, and the integrals of its terms can then be replaced by infinite integrals again with only a transcendantally small error. Thus in fact, one need not worry about the non-uniformity in k^2 of the expansions.

It is now relatively easy to invert the Fourier transforms, using the following:

$$\frac{1}{2\pi}\int_{-\infty}^{\infty} e^{-ikY-ak^2/4}\, dk = (\pi a)^{-\frac{1}{2}}e^{-Y^2/a} \tag{29a}$$

$$\frac{1}{2\pi}\int_{-\infty}^{\infty} e^{-ikY-k^2/4-a|k|}dk = \frac{\pi^{-\frac{1}{2}}}{2}\left[e^{(a-iY)^2}\mathrm{Erfc}(a-iY) + e^{(a+iY)^2}\mathrm{Erfc}(a+iY)\right] \tag{29b}$$

$$\frac{1}{2\pi}\int_{-\infty}^{\infty} e^{-ikY-k^2/4}\cos(ak^2+b)dk = \pi^{-\frac{1}{2}}(1+16a^2)^{-\frac{1}{4}}e^{-Y^2/(1+16a^2)} \cdot \cdot \cos\left[\tfrac{1}{2}\tan^{-1}4a - \frac{4aY^2}{1+16a^2} + b\right] \tag{29c}$$

and

$$\frac{1}{2\pi}\int_{-\infty}^{\infty} e^{-ikY-k^2/4}\cos ak\,dk = \pi^{-\frac{1}{2}}e^{-a^2-Y^2}\cosh 2aY \tag{29d}$$

(See, for instance [Erdelyi et al, Tables of Integral Transforms, McGraw Hill 1954] ; the integrals are also not difficult to evaluate directly.)
(29b) can also be written in real form as

$$\frac{1}{2\pi}\int_{-\infty}^{\infty} e^{-ikY-k^2/4-a|k|}dk = \pi^{-\frac{1}{2}}e^{-Y^2}\, e^{a^2}\cos 2aY\ \mathrm{Erfc}a + 2\pi^{-\frac{1}{2}}\int_0^Y e^{\eta^2}\sin 2a(Y-\eta)d\eta \tag{30}$$

In addition, for the ϵ^2 terms, we need similar integrals with an extra factor of k^2; these can be obtained from the above by differentiating twice with respect to Y:

$$\frac{1}{2\pi}\int_{-\infty}^{\infty} e^{-ikY}k^2e^{-ak^2/4}dk = (\pi a^3)^{-\frac{1}{2}}(2-4Y^2/a)e^{-Y^2/a} \tag{31a}$$

$$\frac{1}{2\pi}\int_{-\infty}^{\infty} k^2e^{-ikY-k^2/4-a|k|}dk = \pi^{-\frac{1}{2}}\Big[(4a^2+2-4Y^2)e^{-Y^2}\, e^{a^2}\cos 2aY\ \mathrm{Erfc}a + 2\pi^{-\frac{1}{2}}\int_0^Y e^{\eta^2}\sin 2a(Y-\eta)d\eta - 4a\pi^{-\frac{1}{2}} + 8aYe^{-Y^2}\Big[e^{a^2}\sin 2aY\ \mathrm{Erfc}a + 2\pi^{-\frac{1}{2}}\int_0^Y e^{\eta^2}\cos 2a(Y-\eta)d\eta\Big]\Big] \tag{31b}$$

$$\frac{1}{2\pi}\int_{-\infty}^{\infty} k^2 e^{-ikY-k^2/4}\cos(ak^2+b)dk = \pi^{-\frac{1}{2}}(1-16a^2)^{-5/4}\, e^{-Y^2/(1+16a^2)}\cdot$$

$$\cdot\left\{\left[2-4Y^2\frac{1-16a^2}{1+16a^2}\right]\cos\left(\tfrac{1}{2}\tan^{-1}4a-\frac{4aY^2}{1+16a^2}+b\right) - 8a\left[1-\frac{4Y^2}{1+16a^2}\right]\sin\left(\tfrac{1}{2}\tan^{-1}4a - \frac{4aY^2}{1+16a^2}+b\right)\right\} \tag{31c}$$

$$\frac{1}{2\pi}\int_{-\infty}^{\infty} e^{-ikY^2-k^2/4}\, k^2\cos ak\, dk = \pi^{-\frac{1}{2}}e^{-a^2-Y^2}\left[(2-4Y^2-4a^2)\cosh 2aY + 4aY\sinh 2aY\right] \tag{31d}$$

Using these, and setting

$$Q = \frac{2nk}{\pi}/(K^2-n^2+J) \tag{32a}$$

(so that $P_o^o = \pi^{\frac{1}{2}}Qe^{-k^2/4}$)

$$\beta^2 = J/|J-n^2| \tag{32b}$$

$$\nu^2 = 4n^4|J-n^2|^{-3} \tag{32c}$$

$$\phi = \tfrac{1}{2}\tan^{-1}\nu|X| - \nu|X|Y^2/(1+\nu^2X^2) + \sqrt{J-n^2}\,x \tag{32d}$$

The inverse transforms of (23) and (24) give:

$$w_o^{(n)} = Q\left\{e^{-Y^2-K|x|}\,\mathrm{sgn}x - (1+\mathrm{sgn}x)(1+\nu^2X^2)^{-\frac{1}{4}}e^{-Y^2/(1+\nu^2X^2)}\cos\phi\right\} \quad (n<n^*) \tag{33a}$$

$$w_o^{(n)} = Q\left\{e^{-Y^2-K|x|} - e^{-Y^2/(1+\nu|X|)} - \sqrt{n^2-J}\,|x|\,(1+\nu|X|)^{-\frac{1}{2}}\,\mathrm{sgn}x\right\} \quad (n>n^*) \tag{33b}$$

$$w_2^{(n)} = Q\frac{1+J/K^2}{K^2-n^2+J}(2-4Y^2)e^{-Y^2-K|x|}\,\mathrm{sgn}x - QJ\frac{K^2-n^2+J}{K^2(J-n^2)^2}\cdot$$

$$\cdot\Big\{(2-4Y^2+4\beta^2\xi^2)e^{-Y^2}\Big[e^{\beta^2\xi^2}\mathrm{Erfc}(\beta|\xi|)\cos 2\beta\xi + 2\pi^{-\frac{1}{2}}\int_0^Y e^{\eta^2}\sin 2\beta|\xi|(Y-\eta)\,d\eta\Big]$$

$$-4\pi^{-\frac{1}{2}}\beta|\xi| + 8\beta|\xi|Ye^{-Y^2}\Big[e^{\beta^2\xi^2}\mathrm{Erfc}(\beta|\xi|)\sin 2\beta|\xi|$$

$$+ 2\pi^{-\frac{1}{2}}\int_0^Y e^{\eta^2}\cos 2\beta\xi(Y-\eta)\,d\eta\Big]\Big\}\,\mathrm{sgn}x$$

$$-Q(1+\mathrm{sgn}x)\frac{n^4-JK^2-J^2}{(J-n^2)^2(K^2-n^2+J)}(1+\nu^2X^2)^{-5/4}e^{-Y^2/(1+\nu^2X^2)}\cdot$$

$$\cdot\Big\{\Big[2-4Y^2\frac{1-\nu^2X^2}{1+\nu^2X^2}\Big]\cos\phi - 2\nu|X|\Big(1-\frac{4Y^2}{1+\nu^2X^2}\Big)\sin\phi\Big\}, \quad (n\le n^*) \qquad (34a)$$

$$w_2^{(n)} = Q\frac{1+J/K^2}{K^2-n^2+J}(2-4Y^2)e^{-Y^2-K|x|}\,\mathrm{sgn}\,x -$$

$$-Q\frac{n^4-JK^2-J^2}{(n^2-J)^2(K^2-n^2+J)}\Big(2-\frac{4Y^2}{1+\nu|X|}\Big)(1+\nu|X|)^{-3/2}e^{-\sqrt{n^2-J}|X|-Y^2/(1+\nu|X|)}\,\mathrm{sgn}x$$

$$-QJ(1+\mathrm{sgn}x)\frac{K^2-n^2+J}{K^2(n^2-J)^2}e^{-Y^2-\beta^2\xi^2}\Big[(2-4Y^2-4\beta^2\xi^2)\cosh(2\beta\xi Y)$$

$$+ 4\beta\xi\sinh(2\beta\xi Y).\Big] \qquad (n>n^*) \qquad (34b)$$

(33a) exhibits the lee waves seen at large positive x, the function ϕ of (32d) giving the phase. If X is large enough that $\nu X \gg 1$, the lines of constant phase are approximately the hyperbolas

$$Y^2 - \frac{(J-n^2)^{\frac{1}{2}}}{\epsilon^2\nu}\Big((\nu X)^2+1\Big) + (\phi-\tfrac{\pi}{4})\,\nu X = 0$$

which have asymptotes of slope

$$\frac{dy}{dx} = \epsilon\frac{dY}{dx} = \pm\sqrt{\nu}\,(J-n^2)^{\frac{1}{4}}$$

A picture of some lines of constant phase computed from (32a) for the case $(J-n^2)^{\frac{1}{2}}/\varepsilon^2\nu = 10$ is shown in Figure 1. Of course, if there is more than one lee wave mode ($n_*>1$), the asymptotic solution will be a sum of such terms, and the picture will be more complex.

The inverse transforms for the other components of the flow can be obtained in the same way from equations (25) and (28). We give only the results pertinent to u and v up to $O(\varepsilon)$.

$$u^{(o)} = \frac{2}{\pi} e^{-Y^2} \left\{ e^{-K|x|} - \frac{\varepsilon}{K} \left[2e^{\xi^2} \mathrm{Erfc}\xi \cdot \right.\right.$$

$$\cdot (Y\sin 2\xi Y - \xi\cos 2\xi Y) + 2\pi^{-\frac{1}{2}} e^{Y^2}$$

$$\left.\left. -4\pi^{-\frac{1}{2}} \int_0^Y e^{\eta^2} \left[Y\cos 2\xi(Y-\eta) - \xi\sin 2\xi(Y-\eta) \right] d\eta \right] \right\} + O(\varepsilon^2) \qquad (35a)$$

$$u^{(n)} = \frac{Q}{n} \left\{ \frac{K^2+J}{K} e^{-Y^2 - K|x|} + (1+\mathrm{sgn}x) \frac{n^2}{\sqrt{J-n^2}} (1+\nu^2X^2)^{-\frac{1}{4}} \cdot \right.$$

$$\cdot e^{-Y^2/(1+\nu^2X^2)} \sin\phi - \varepsilon\beta^3 \frac{K^2-n^2+J}{K^2} e^{-Y^2} 2e^{\beta^2\xi^2} \mathrm{Erfc}(\beta|\xi|) \cdot$$

$$\cdot (Y\sin 2\beta|\xi| Y - \beta|\xi|\cos 2\beta\xi Y) + 2\pi^{-\frac{1}{2}} e^{Y^2}$$

$$\left. -4\pi^{-\frac{1}{2}} \int_0^Y e^{\eta^2} \left[Y\cos 2\beta\xi(Y-\eta) - \beta\xi\sin 2\beta\xi(y-\eta) \right] d\eta \right\} + O(\varepsilon^2)$$

$$(o<\eta\leq\eta_*) \qquad (35b)$$

$$u^{(n)} = \frac{Q}{n} \left\{ \frac{K^2+J}{K} e^{-Y^2 - K|x|} - \frac{n^2}{\sqrt{n^2-J}} (1+\nu|X|)^{-\frac{1}{2}} e^{-\sqrt{n^2-J}|x| - Y^2/(1+\nu|X|)} \right.$$

$$\left. + \varepsilon(1+\mathrm{sgn}x) 2\beta^3 \frac{K^2-n^2+J}{K^2} e^{-\beta^2\xi^2 - Y^2} \left\{ \beta|\xi|\cosh 2\beta\xi Y - Y\sinh 2\beta|\xi| Y \right\} \right\} + O(\varepsilon^2)$$

$$(n>n_*) \qquad (35c)$$

$$v^{(o)} = \frac{4}{\pi K} e^{-Y^2} \Big\{ Ye^{-K|x|} - e^{\xi^2}\mathrm{Erfc}|\xi|\,(Y\cos 2\xi Y + \xi \sin 2\xi Y)$$

$$-2\pi^{-\frac{1}{2}} \int_o^Y e^{\eta^2} \left[Y\sin 2|\xi|(Y-\eta) - |\xi|\cos 2\xi(Y-\eta) \right] d\eta \Big\} \, \mathrm{sgn}x + O(\epsilon^2) \qquad (36a)$$

$$v^{(n)} = \frac{2Q}{n} \Big\{ e^{-Y^2}\,\mathrm{sgn}x \left[\frac{K^2+J}{K^2} Ye^{-K|x|} - \beta^2 \frac{K^2-n^2+J}{K^2} \Big\{ e^{\beta^2\xi^2}\mathrm{Erfc}\beta|\xi| \cdot \right.$$

$$\cdot (Y\cos 2\beta\xi Y + \beta\xi \sin 2\beta\xi Y) + 2\pi^{-\frac{1}{2}} \int_o^Y e^{\eta^2} (Y\sin 2\beta|\xi|(Y-\eta)$$

$$\left. -\beta|\xi|\cos 2\beta\xi(Y-\eta) \Big\} d\eta \right] + (1+\mathrm{sgn}x) \frac{n^2}{J-n^2} (1+\nu^2X^2)^{-5/4} \cdot$$

$$\cdot Ye^{-Y^2/(1+\nu^2X^2)} (\cos\phi - \nu|X|\sin\phi) + O(\epsilon^2) \Big\} \quad , \; (o<n\leq n^*) \qquad (36b)$$

$$v^{(n)} = \frac{2Q}{n} \Big\{ \frac{K^2+J}{K^2} Ye^{-Y^2-K|x|}\,\mathrm{sgn}x - \frac{n^2}{n^2-J} e^{-\sqrt{n^2-J}\,|x|} \cdot$$

$$\cdot (1+\nu|X|)^{-3/2} Ye^{-Y^2/(1+\nu|X|)}\,\mathrm{sgn}x + (1+\mathrm{sgn}x)\beta^2 \frac{K^2-n^2+J}{K^2} \cdot$$

$$\cdot e^{-Y^2-\beta^2\xi^2} \Big(Y\cosh 2\beta\xi Y - \beta\xi \sinh 2\beta\xi Y) \Big\} + O(\epsilon^2) \quad , \; (n>n^*) \; . \qquad (36c)$$

We now must see how to improve the convergence of the sine series for w so that it can be used for computation. Since $Q\nu \sim -\frac{2K}{n\pi}$ for large n (See (32a), and $\nu\nu$ 2/n, we see from (33b) that

$$w_o^{(n)} = -\frac{2K}{\pi n} e^{-Y^2}(e^{-K|x|}-e^{-n|x|})\operatorname{sgn} x +$$

+ terms of order n^{-2} or smaller. (Of course the series $\Sigma\frac{1}{n}e^{-n|x|}\sin nz$ is ultimately rapidly convergent if $x\neq o$, but the approximation by a moderate number of terms becomes poor as $x\to o$.)

However, the series with the asymptotic form as coefficients can be summed exactly, so by removing this part we are left with a series which converges rapidly enough to be useful. The power series $\sum_1^\infty Z^n/n$ converges to -log(1-Z) inside the unit circle in the complex Z plane, the logarithm being defined as 0 at Z=0 and with a branch cut extending to the right from Z=1. By Abel's theorem, it also converges to this same sum on the unit circle too, except at Z=1. Setting $Z=e^{-|x|+iz}$ this gives

$$\sum_1^\infty e^{-n|x|}e^{inz}/n = -\log(1-e^{-|x|+iz})$$

$$\therefore \sum_1^\infty e^{-n|x|}\frac{\sin nz}{n} = \operatorname{Im}\left\{-\log(1-e^{-|x|}\cos z - ie^{-|x|}\sin z)\right\}$$

$$= \tan^{-1}\left(\frac{e^{-|x|}\sin z}{1-e^{-|x|}\cos z}\right) = \tan^{-1}\frac{\sin z}{e^{|x|}-\cos z}$$

In particular, for x=o, we recover the familiar series

$$\sum_1^\infty \frac{\sin nz}{n} = \tan^{-1}\frac{\sin z}{1-\cos z} = \tan^{-1}\cot z/2 = \tfrac{1}{2}(\pi - z)$$

Thus we have

$$\sum_1^\infty\left(e^{-K|x|}-e^{-n|x|}\right)\frac{\sin nz}{n} = e^{-K|x|}\frac{\pi-z}{2} - \tan^{-1}\left(\frac{\sin z}{e^{|x|}-\cos z}\right) \qquad (37)$$

Let us set

$$w_o^{(n)} = \operatorname{sgn} x \, \frac{2K}{\pi} \, e^{-Y^2} \left(\frac{e^{-K|x|} - e^{-n|x|}}{n} \right) + w_o^{(n)} \qquad (38)$$

Then we have

$$w^{(o)} = -\frac{2K}{\pi} e^{-Y^2} \left[e^{-K|x|} \frac{\pi - z}{2} - \tan^{-1} \left(\frac{\sin z}{e^{|x|} - \cos z} \right) \right] \operatorname{sgn} x$$

$$+ \sum_1^\infty \hat{w}_o^{(n)} \sin nz$$

and the series in (39) should converge rapidly enough for direct numerical evaluation.

Investigation of the asymptotic behaviour of the terms in $w^{(n)}$ (34b) shows that they decrease like n^{-3}, so the series may there be used directly. (35c) shows that for large n

$$u^{(n)} \sim \frac{2K}{\pi\eta} e^{-n|x| - Y^2} .$$

Thus we set

$$\hat{u}^{(n)} = -\frac{2K}{\pi\eta} e^{-Y^2 - n|x|} + u^{(n)} \qquad (n \geq 1) \qquad (40)$$

Since in this case we have a cosine series, we use

$$\sum_1^\infty e^{-n|x|} \frac{\cos nz}{n} = \operatorname{Re} \left\{ -\log(1 - e^{-|x|} \cos z - i e^{-|x|} \sin z) \right\}$$

$$= -\tfrac{1}{2} \log \left(1 - 2e^{-|x|} \cos z + e^{-2|x|} \right)$$

and so

$$u = -\frac{K}{\pi} \log \left(1 - 2e^{-|x|} \cos z + e^{-2|x|} \right) e^{-Y^2} + \frac{u^{(o)}}{2} + \sum_1^\infty \hat{u}^{(n)} \cos nz \qquad (41)$$

The terms $v^{(n)}$ already decrease like $\frac{1}{n^2}$.

IV RESULTS AND DISCUSSION

Numerical evaluation of w and v is made for both the single mountain ridge and the mountain-valley cases, under combination of the following conditions:

h_o = 1 Km	$U = 10\ msec^{-1}$
ϵ = 0.2	K = 1.25
J = 2.0, 7, 13, and 20	H = 3 Km

Based on the formula for a single mountain ridge shown in (3), the corresponding formula for the mountain-valley terrain case can be written in non-dimensional form as

$$\frac{h}{h_o} = \left[e^{-K|x-1.50|} + e^{-K|x+1.50|} \right] e^{-Y^2}$$

in which the valley width or the separation of ridges is three non-dimensional unit of length, i.e., 9 Km in actual distance. For the single mountain case, the peak of the ridge is placed at the origin. For the mountain-valley case, the valley head is placed at the origin, and peaks of the ridge are at x=±1.50, y=o. For the parameters used here, the valley head has the elevation of about 300 m above the horizontal plain. The abscissa x and ordinate y in the graphs concerning the vertical velocity distributions are dimensionless and each corresponding unit is equal to 3 Km for x and $\frac{\pi}{6}$ Km for z. The velocities are also non-dimensional. The vertical velocity w of unity corresponds to $3.33\ msec^{-1}$ for the value of the parameters used in the present model. For the figures regarding the distribution of the horizontal velocity component, v, the ordinate Y is also dimensionless and Y = 1 corresponds to y = 15 Km. The velocity v of unity corresponds to $2/3\ msec^{-1}$. The horizontal velocity component normal to the mountain ridge is not of much interest here and is thus not calculated.

Figures 2 and 3 show the vertical cross-section of the vertical velocity distribution $w(x,z)$, at Y=0 over a single mountain, corresponding to J = 2.0, and the horizontal cross-section of $w(x,Y)$ at $z = \frac{\pi}{3}$ Km for J = 2.0 respectively. Both clearly show that the flow is down slope in the lee of the ridge. Above the mountain ridge and in the lee phase retardation takes place with height. There is very little retardation, however, farther away from the mountain, as shown in Figure 3.

The horizontal distribution of w for the case J = 2.0 is shown in Figure 3. The phase line in the horizontal plane at the z = 1.04 Km level is concave toward the downwind direction. Bow-shaped or crescent shaped clouds will develop as the manifestation of the vertical motion field where there is enough moisture. Such clouds were reported by Abe (1941). A crescent-shaped clear area that developed over an overcast area with low stratus clouds was recently reported by Edinger and Wurtele (1972). Figure 4 shows the vertical cross-section of v at Y = 1 (15 Km) from the valley peak of the ridge.

For Richardson number J = 10, the Brunt-Väisälä frequency is about 10^{-2}, which is the approximate value for the case of the normal atmosphere. Thus a smaller J means that the atmosphere is less stable. As can be seen from Figures 5 to 8, the phase retardation is more pronounced in the more stable case when J = 20 (Figure 8) than in the less stable case (Figure 5). The higher J will allow high wave modes to come into play. This is clearly shown in these graphs. It is of interest to compare Figures 2 and 5 in which the basic conditions are exactly the same, except for the two mountains. The vertical velocity distributions for the two mountain case is quite different from the single mountain case. The superposition of the wave solution for each single mountain at such a valley width used here leads to the damping. However, the downslope motions still take place in the lee slopes, and the upslope motion in the windward slopes of each mountain. The horizontal wave lengths for Figures 6 and 8 have been shortened somewhat.

Next, let us look at Figures 12 to 14, which depict the vertical cross-section of the wind component parallel to the valley or the ridges at Y = 1. These results are reported for the first time. Figures 12 to 14 show different J's, varying from J = 7 to 20. A considerable increase in J will raise the wave mode. The stronger the stability is, the more difficult it is for the air to move upward. Consequently strong horizontal motion will go around the mountain. Above the valley, the up-valley flow (negative v in the graphs) increases with J and the center of maximum v descends to about the 1.5 Km level at Y = 1. The wind component v will change from down-valley into up-valley at about the 600 m level. In the daytime near valley floors, wind usually blows toward the up-valley direction. Because the down-valley flow discussed above due solely to the lee wave effect persists all the time, it will counteract the thermally induced up-valley winds so that the resultant wind becomes weaker than the normal case. During the night, the down-valley wind attributed to the lee wave effect will strengthen the thermally induced down-valley wind. These results are in very good qualitative agreement with the valley wind observation made in Vermont valleys which have about the same valley width besides a similar wind vector at the 1 Km level as used in the example here, by the New York Univ. Group (Davidson et al., 1958,1963). They have claimed that the case for existence of nighttime down-valley wind was obvious and immediately convincing while the case for existence of its daytime up-valley wind was weak.

Farther in the down-valley direction about 10 Km in the lee, strong confluent flow reaches the surface level at Y = 1. The component of the velocity v, in the direction parallel to the valley or ridges in the lee is closely related to the down-slope lee wave motion. Because the flow in general is down-slope and the horizontal velocity component, u, is maximum near the upper portion of the lee slope, the flow has to force the v component into the down-valley direction from the valley head. For a valley width that is twice or three times the size of the present one (18-25 Km) used for illustrations, the situation may be just opposite, as can be seen from the distribution of v at a position near x=7. The maximum up-valley flow is found less than 500 m above the valley floor and the maximum down-valley wind is found at the 1.7 Km level. Some observations reported opposite to that by the NYU Group may have been conducted near valley center at a site in a wider valley.

Some more interesting results can be found in Figure 15, which shows the distribution of the wind component in the vertical Y-z plane on the valley axis (x = 0) for J = 20. Note that near the z = 0.10 level (∿ 500 m), v changes from down-valley flow into up-valley flow. The flow becomes stronger going away from the valley head at Y = 0, indicating that the downward flow from the valley slope on the upwind direction (ridge at x = 1.50) turns toward the down-valley direction and enhances the thermally induced drainage wind. This indeed has also offered an explanation as to why the maximum down-valley winds are usually found near the valley mouth, and the height of the maximum down-valley wind in the valley increases as the down-valley distance increases. It appears that the results obtained here are in good qualitative agreement with observations and the solutions have depicted the basic physics behind these puzzling and interesting phenomena reported by Davidson et al.,(1958, 1963) and studied analytically from another point of view by Tang (1968).

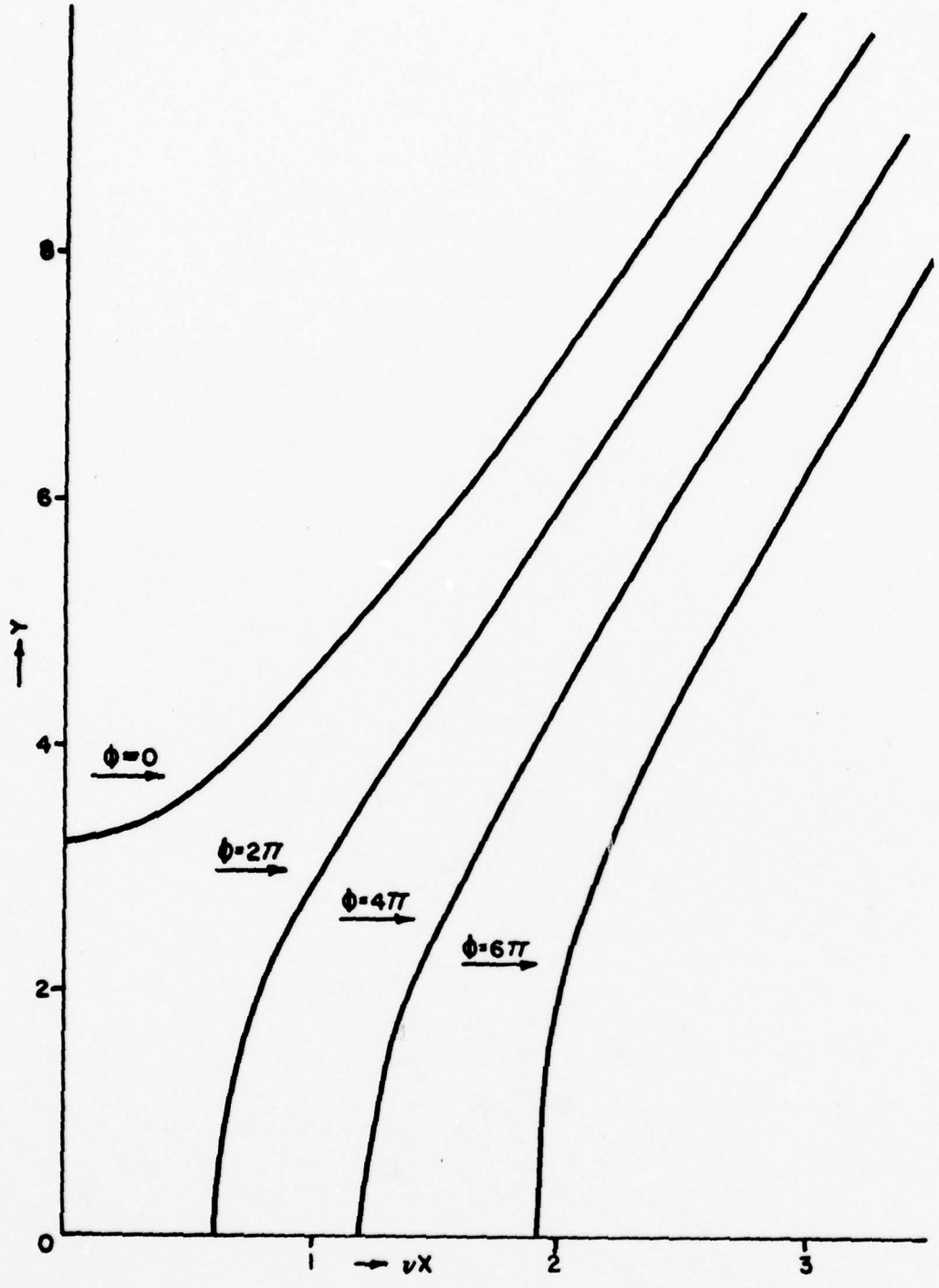

Figure 1. Phase lines of the zeroth order vertical velocity solution for the case $(J-n^2)^{\frac{1}{2}}/\varepsilon^2\nu = 10$.

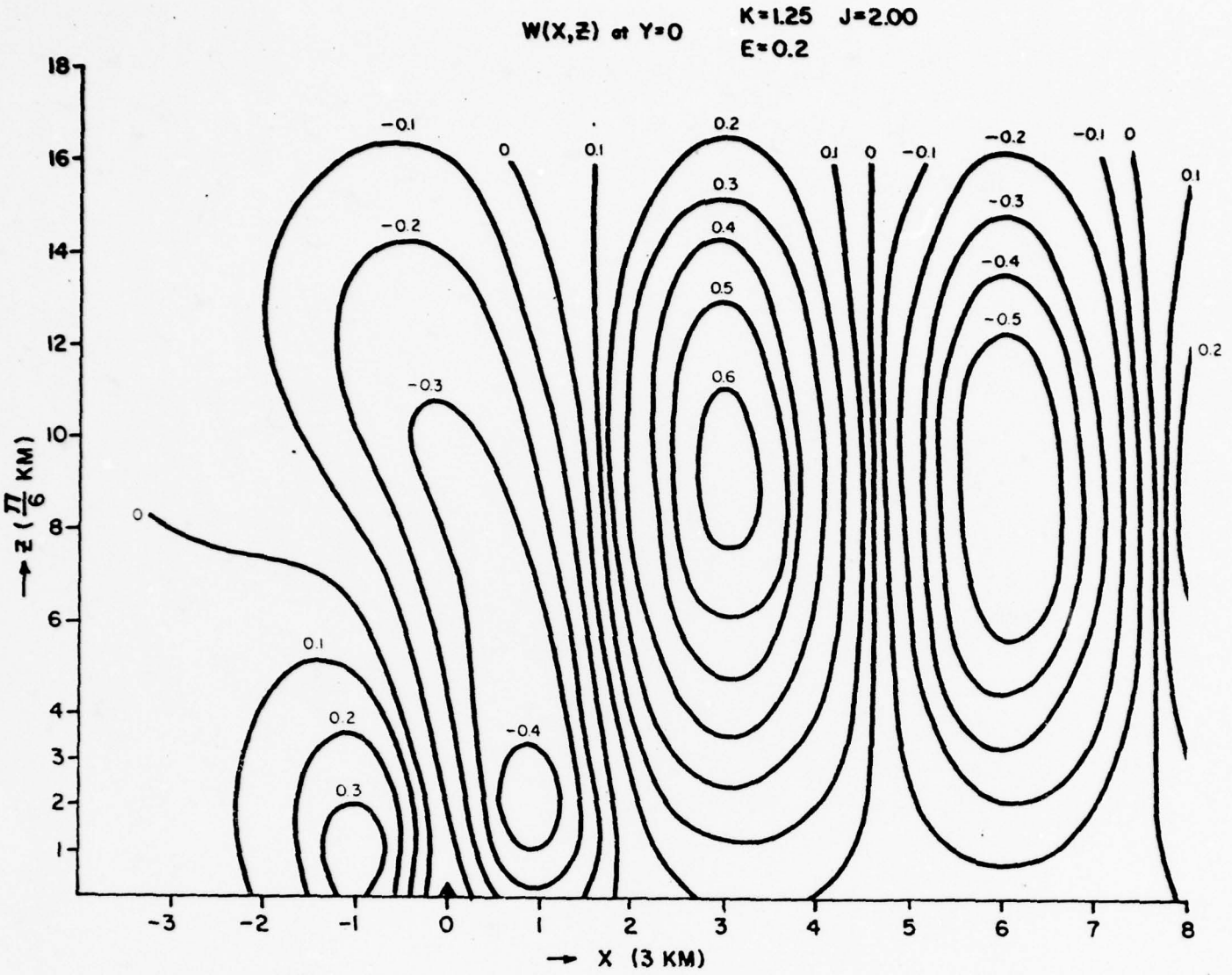

Figure 2. The cross-section of the vertical velocity field W(x,z) for a single mountain at Y = o for ε - 0.2 K = 1.25, and J = 2.0. The mountain is situated at x = o. The ordinate and abscissa are non-dimensional and each unit of them corresponds to $\frac{\pi}{6}$ Km and 3 Km respectively. Y = 1 corresponds to 15 Km. The non-dimensional vertical velocity of unity is equivalent to 3.33 m sec^{-1}.

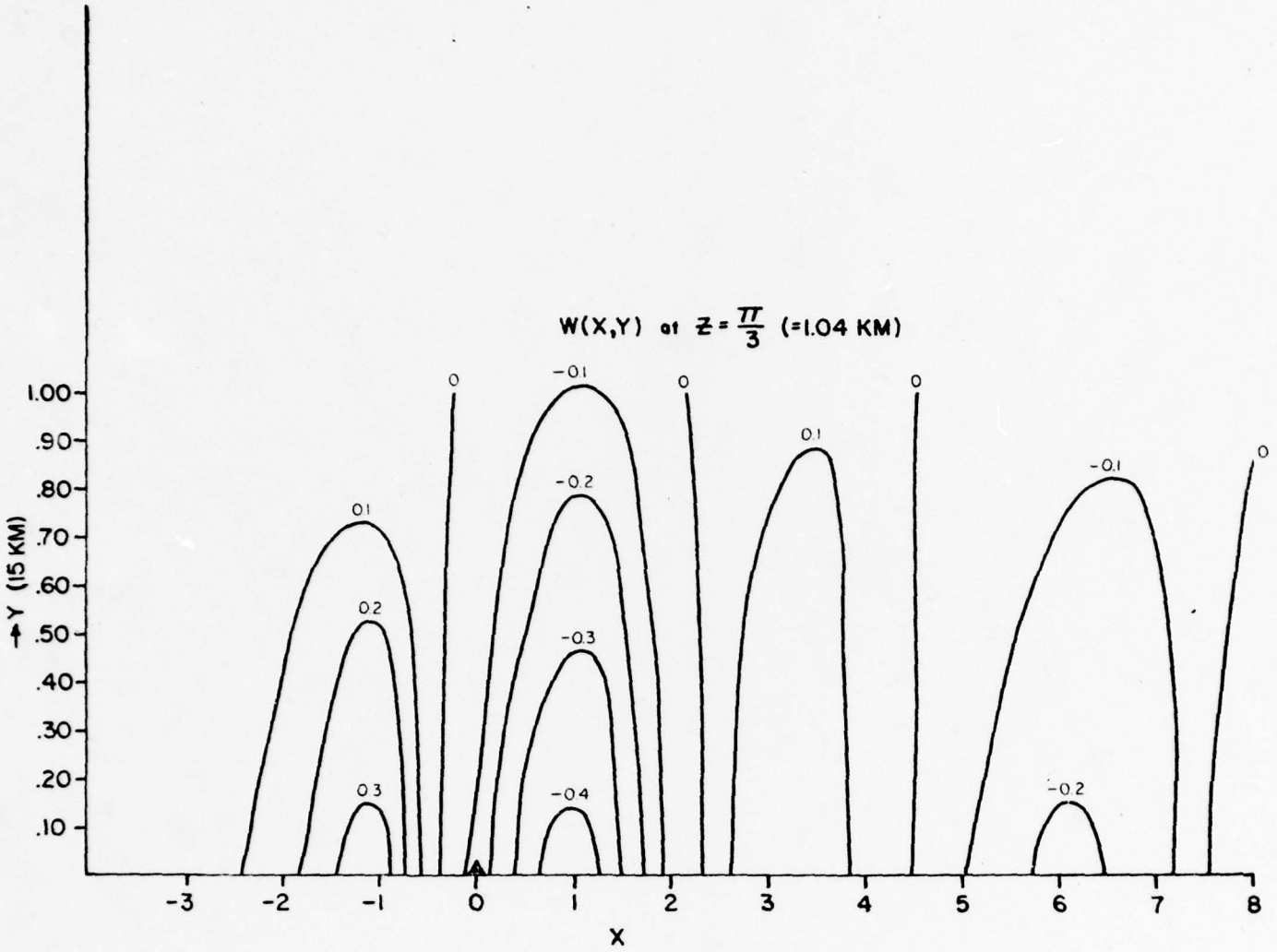

Figure 3. The vertical velocity distribution W(x,Y) on a horizontal plane at the level $z = \frac{\pi}{3}$ Km (same parameters and units as used in Figure 2).

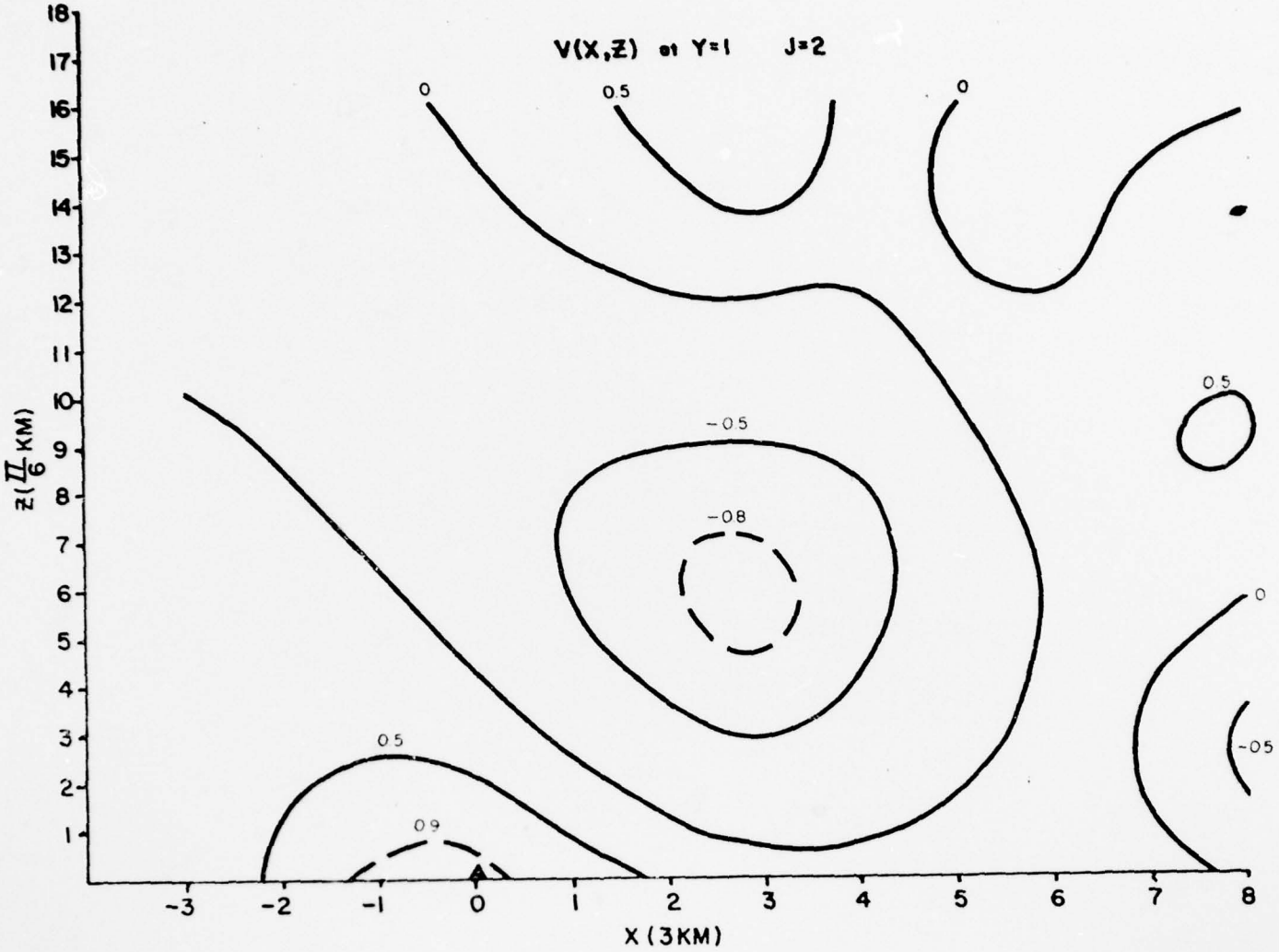

Figure 4. The horizontal velocity component parallel to the ridge lines or along the valley, v(x,z) at Y = 1. (The dimensionless v of unity corresponds to 0.66 m sec^{-1} and other units are same as in Figure 2.)

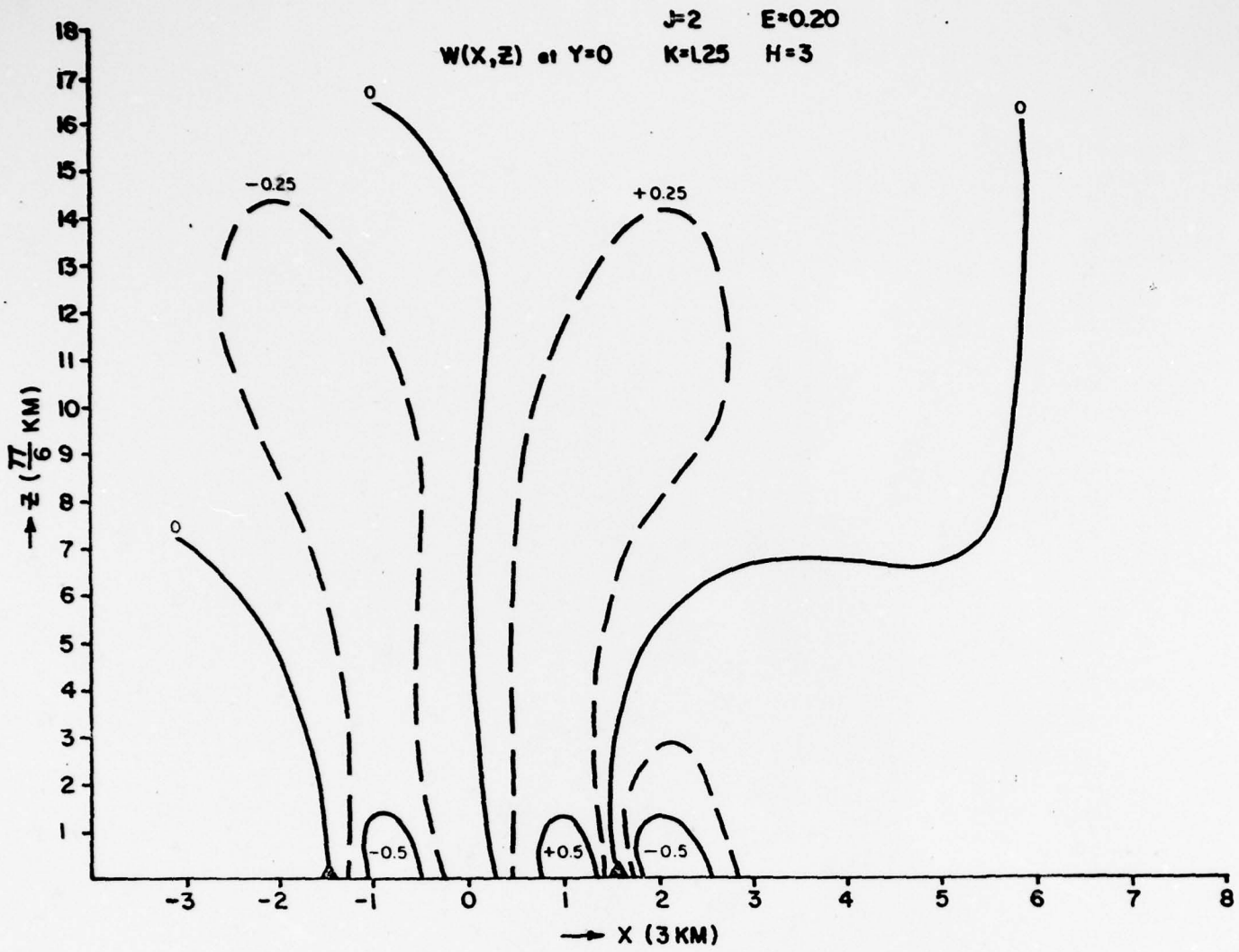

Figure 5. The vertical cross-section of the vertical velocity over mountain-valley terrain at Y = 0 for J = 2.

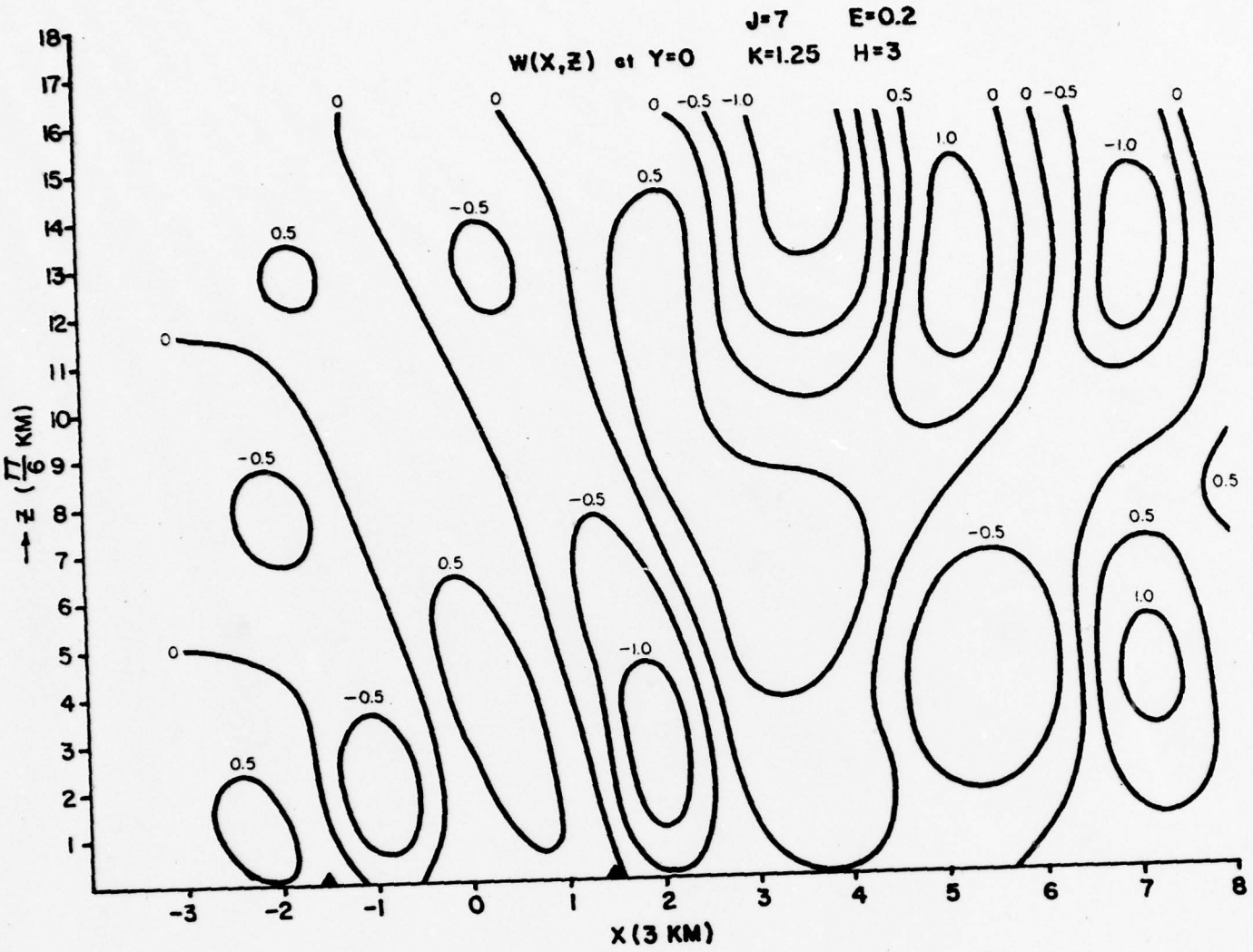

Figure 6. The vertical cross-section of the vertical velocity over mountain-valley terrain at Y = 0 for J = 7.

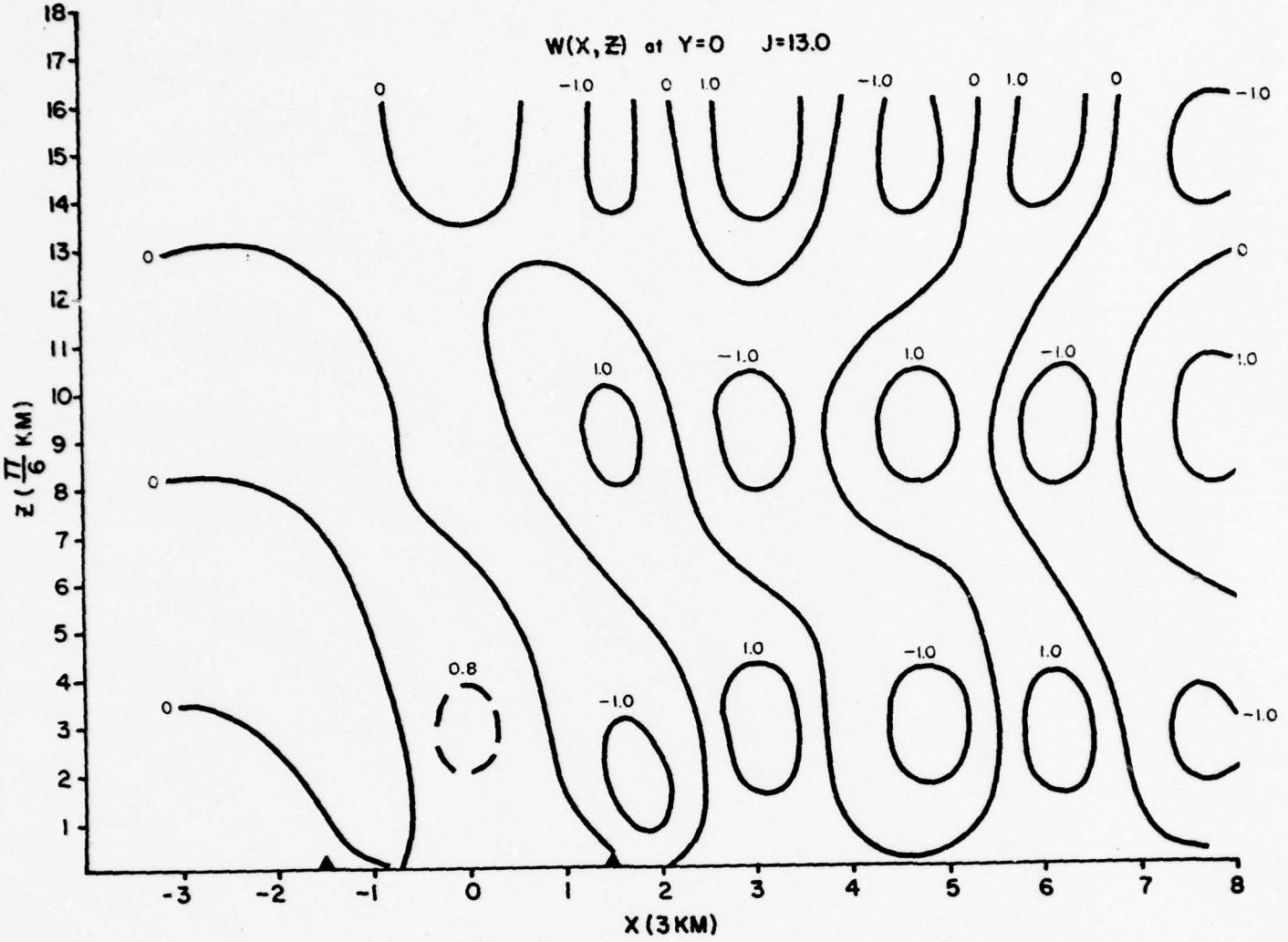

Figure 7. The vertical cross-section of the vertical velocity over mountain-valley terrain at Y = 0 at J = 13.

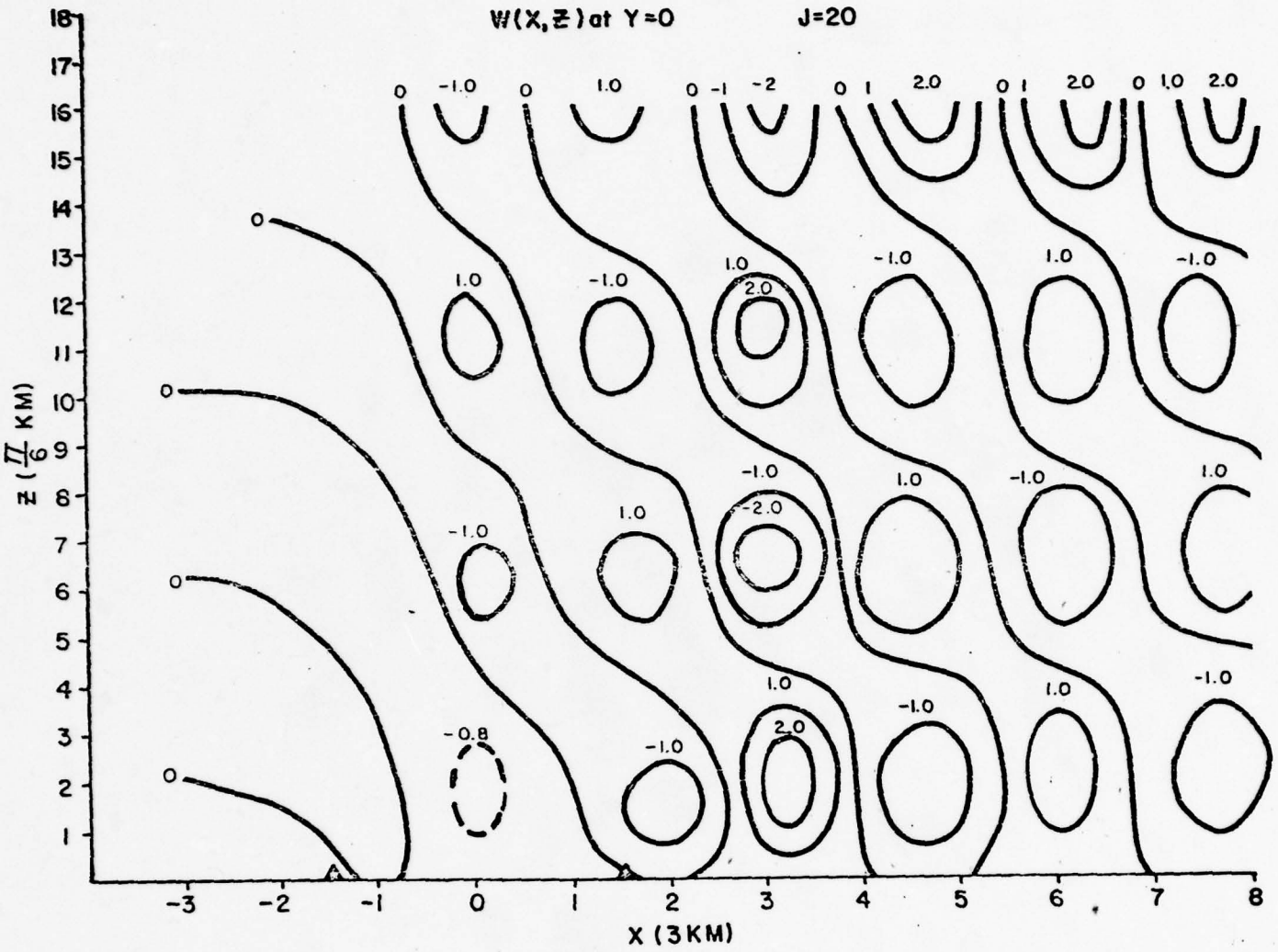

Figure 8. The vertical cross-section of the vertical velocity over mountain-valley terrain at Y = 0 for J = 20.

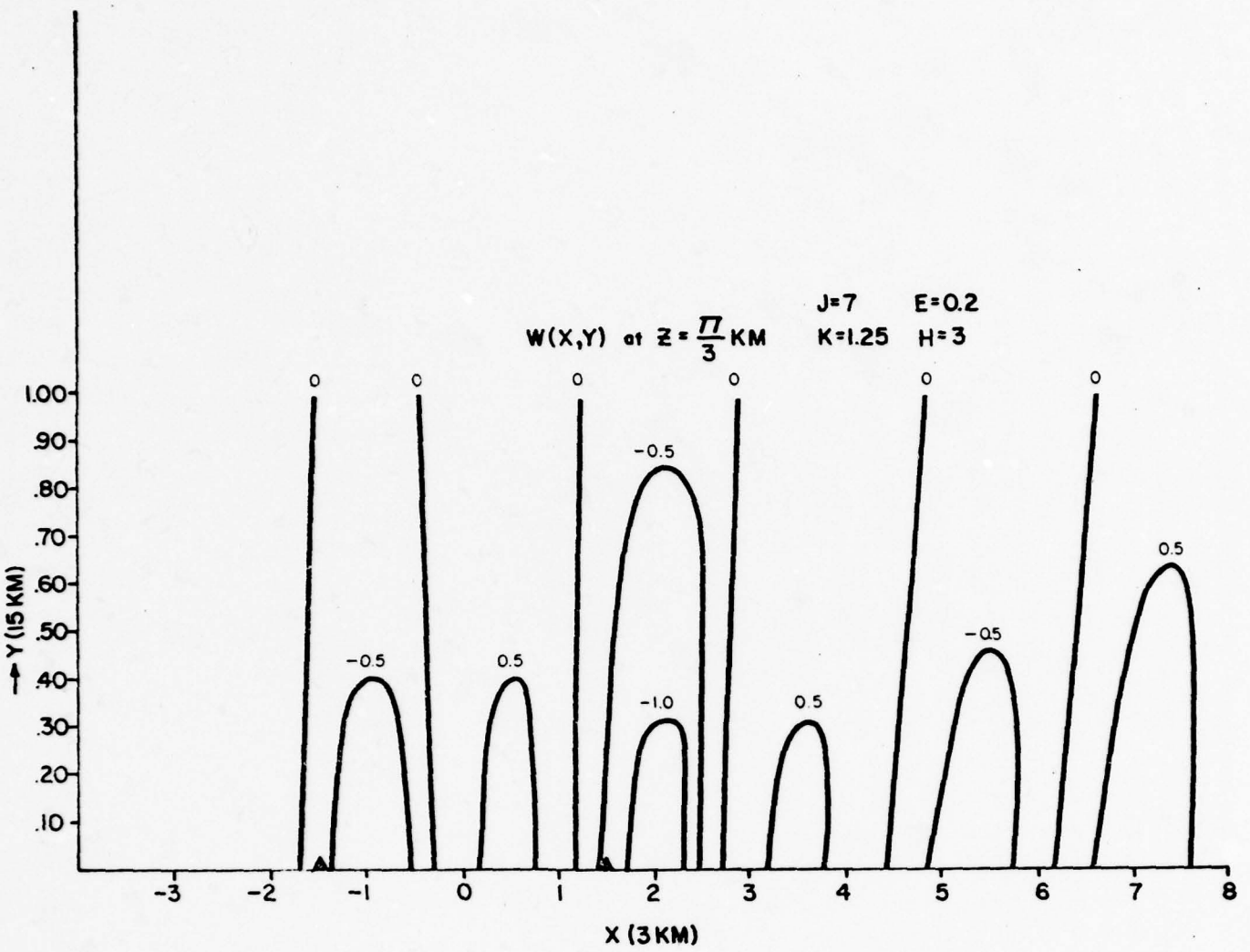

Figure 9. The vertical velocity distribution W(x,Y) on a horizontal plane at the level $z = \frac{\Pi}{3}$ over the mountain-valley terrain for J = 7. (See units in Figure 2.)

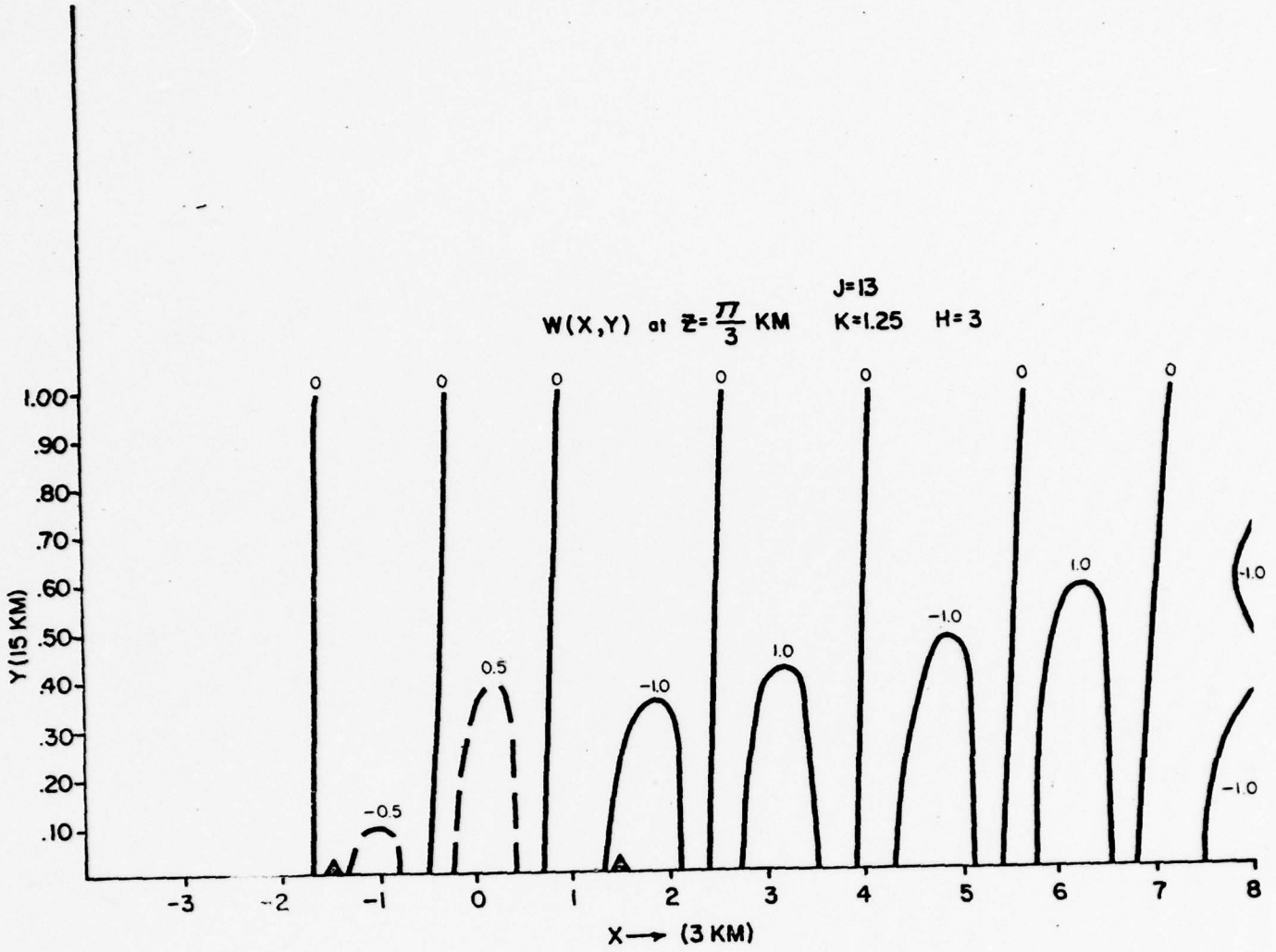

Figure 10. The vertical velocity distribution W(x,Y) on a horizontal plane at the level $z = \frac{\Pi}{3}$ over the mountain-valley terrain for J = 13. (See units in Figure 2.)

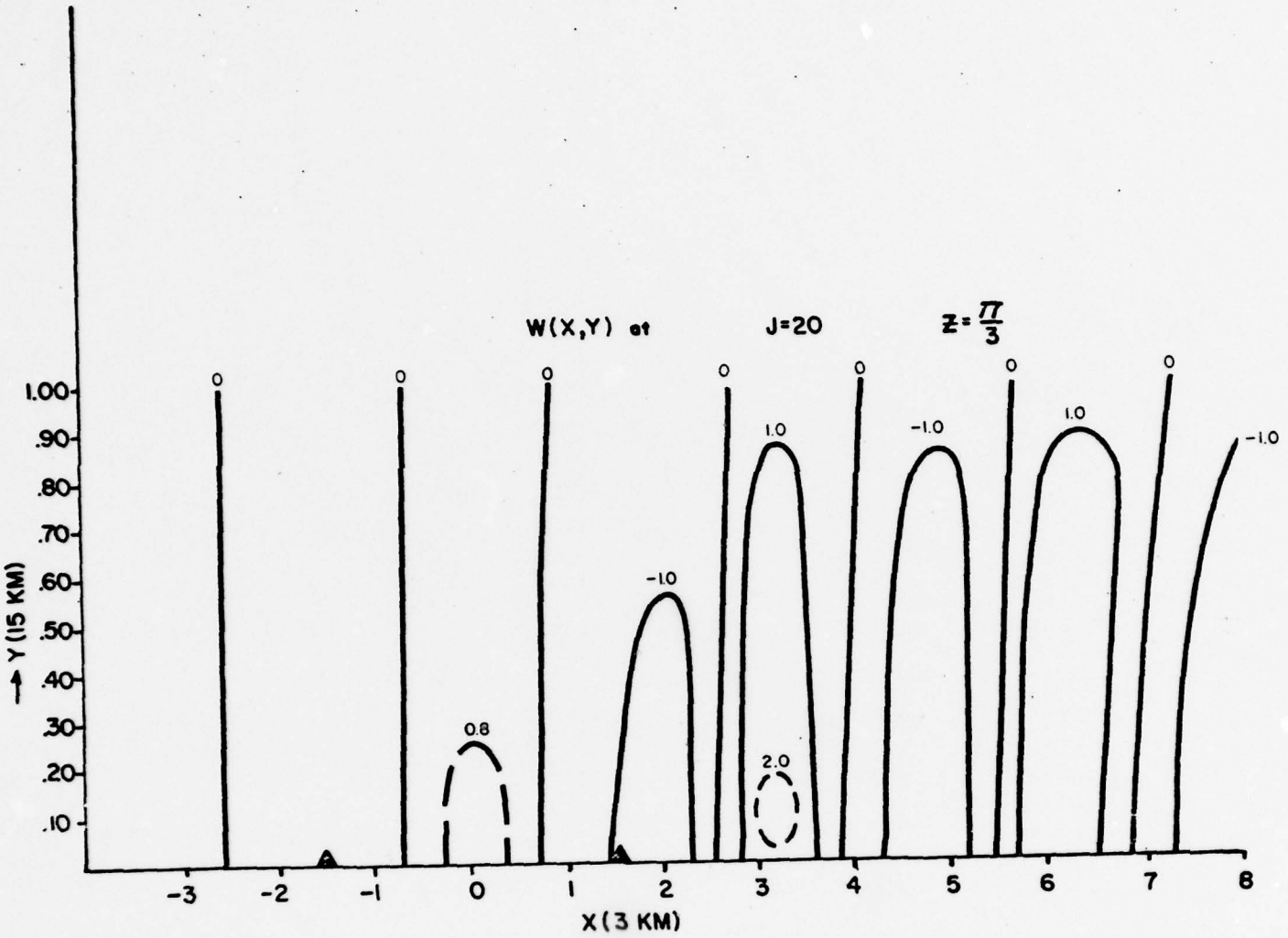

Figure 11. The vertical velocity distribution W(x,Y) on a horizontal plane at the level $z = \frac{\Pi}{3}$ over the mountain-valley terrain for J = 20. (See units in Figure 2.)

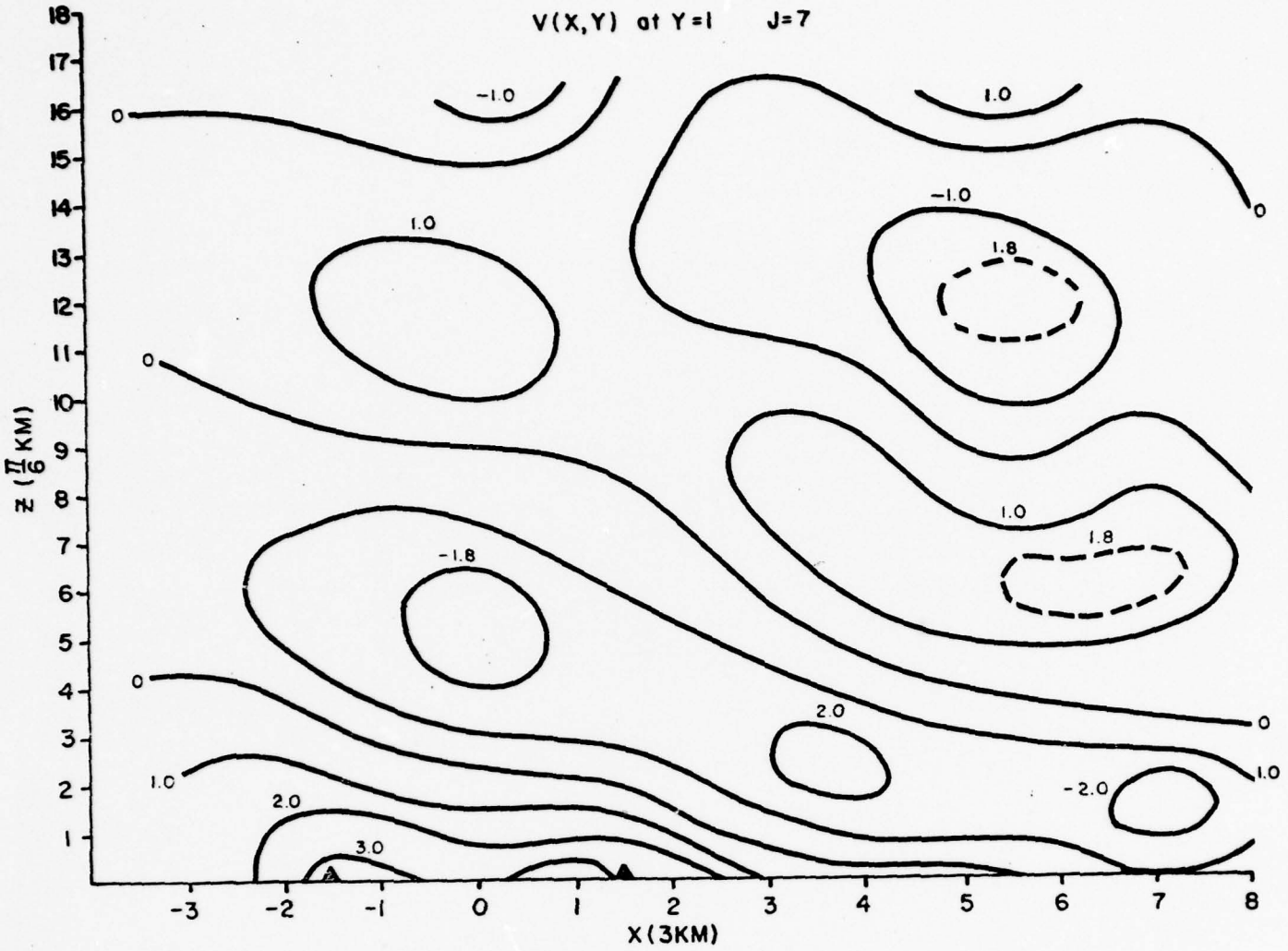

Figure 12. The horizontal velocity component parallel to the ridge lines or along the valley v(x,z) at Y = 1 for J = 7. (See parameter and units in Figure 4.)

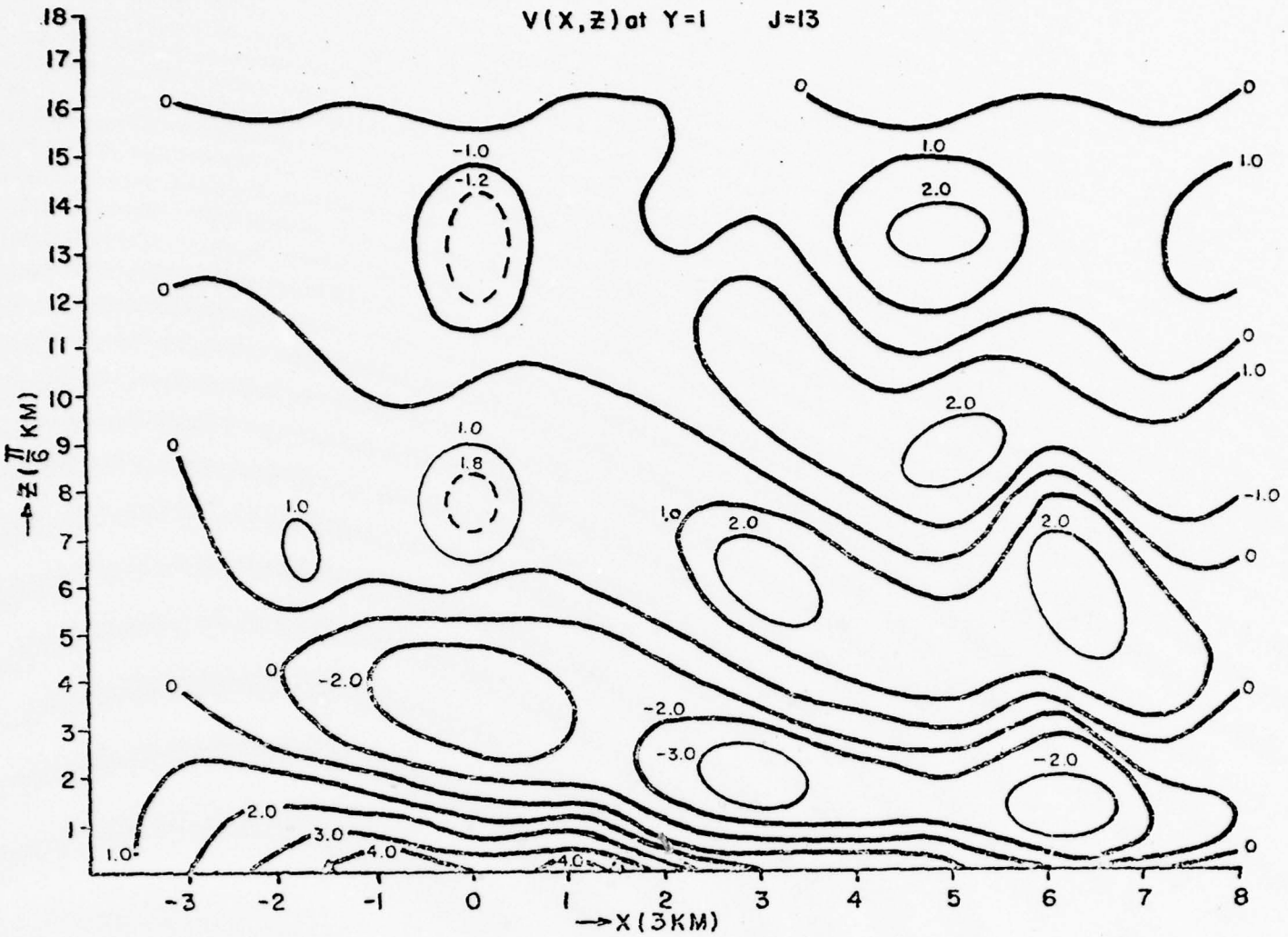

Figure 13. The horizontal velocity component parallel to the ridge lines or along the valley v(x,z) at Y = 1 for J = 13. (See parameter and units in Figure 4.)

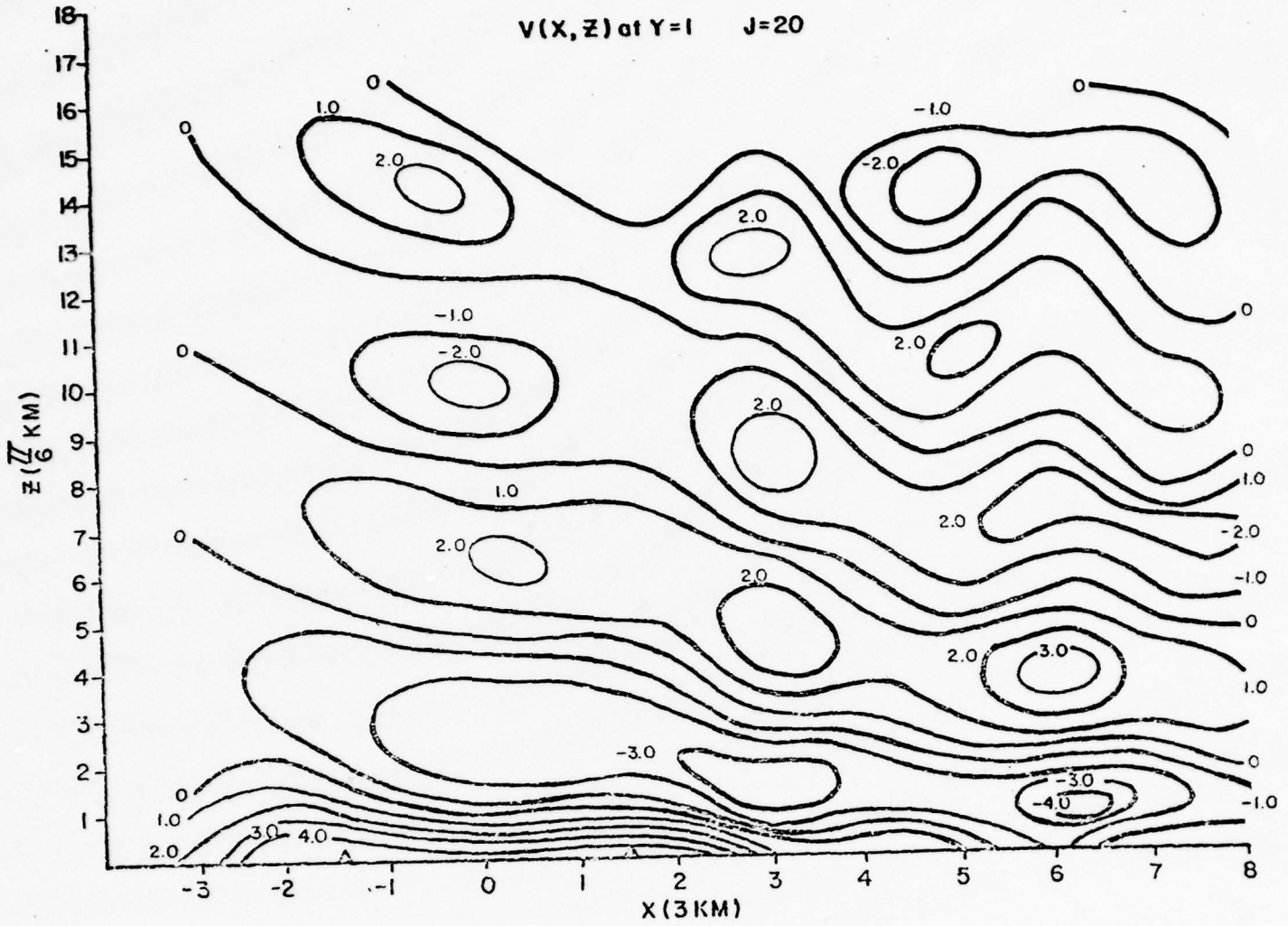

Figure 14. The horizontal velocity component parallel to the ridge lines or along the valley v(x,z) at Y = 1 for J = 20. (See parameter and units in Figure 4.)

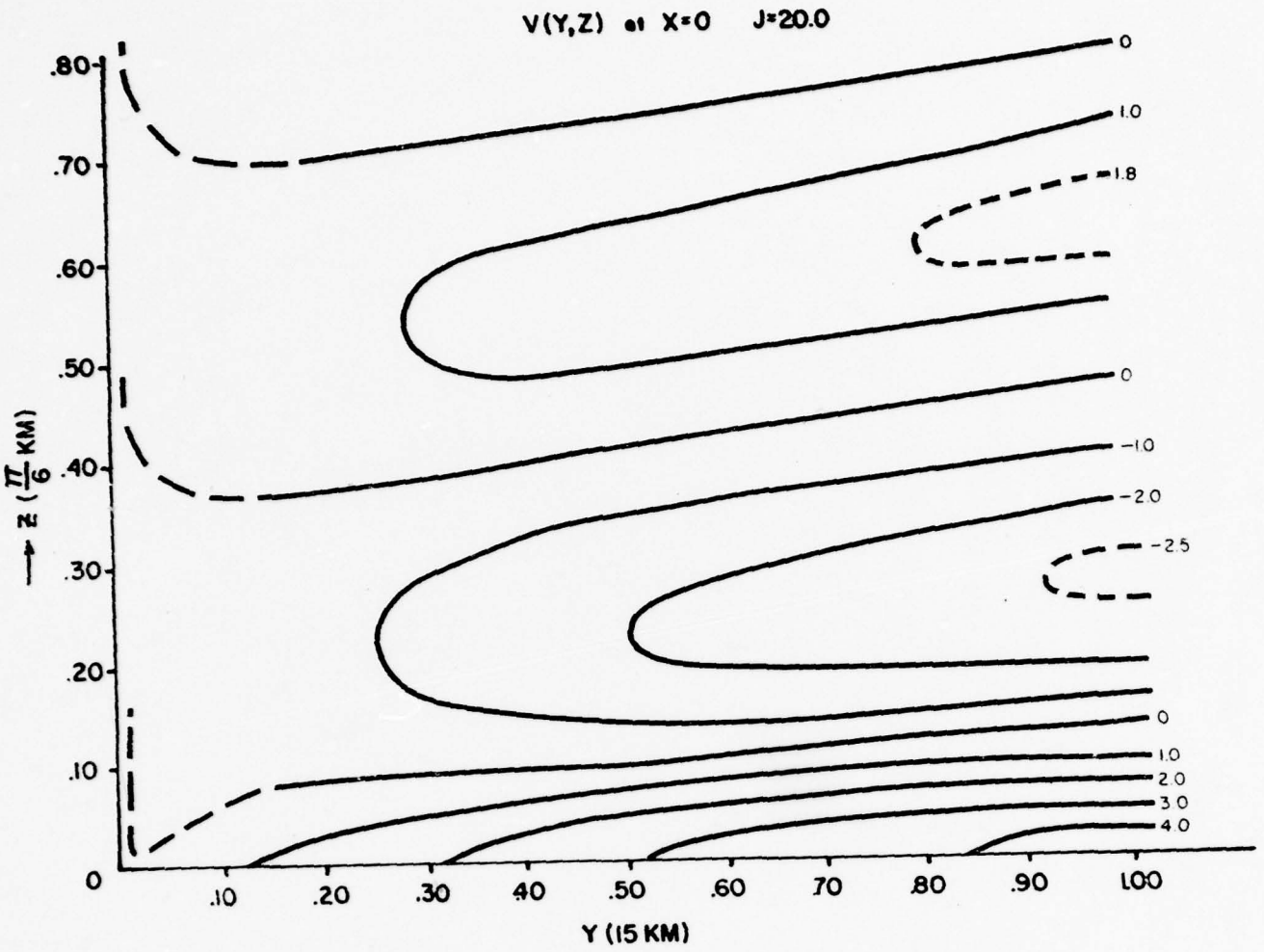

Figure 15. Distribution of v(Y,z) on the valley axis (x = 0) for J = 20. (See parameters and units in Figure 4.)

V CONCLUSIONS AND RECOMMENDATIONS

Study of the flow over and around a truly three-dimensional mountain ridge of finite length and typical mountain-valley terrains has been a difficult task owing to the complicated mathematics involved. The present study has utilized the multiple scaling approach to seek representative solutions converging uniformly, based on a simple linearized model. The present model is different from previous studies in that the solutions are valid for large down-wind distances as well as in the near region. The linear solutions can be superimposed to obtain solutions for the flow over typical mountain-valley cases. Three-dimensional solutions have been obtained which enable us to understand better how the three-dimensional lee wave affects the valley wind system. The solutions explain why a valley with width of about 10 Km may produce a weak up-valley wind during the day and strong down-valley flow during the night. They have also provided an explanation of the increasing of the intensity and the height of the maximum down-valley wind during the night as the down-valley distance increases. The results obtained here are in agreement with observation available and other findings. The size of the valley width and the height of the ridges lines are important factors.

In this study we have developed a model based on a relatively simple assumption in which a constant basic wind field is used to avoid complication in addition to the three-dimensionality in the beginning. It is expected a multiple-layer analytical model with vertical wind shear and different thermal stratifications can be constructed and can extend into the higher atmosphere to include the stratosphere. The thermal boundary layer interaction problem can be attacked in a more or less similar fashion. With the knowledge of truly three-dimensional flow over and around mountain-valley terrain and, in addition, the further analytical study to be done, we can understand much better the interaction between the stratified meso-scale flow forced by the topography and the thermally induced boundary layer flow. At the same time, an investigation with an improved numerical model based upon the work we have developed earlier can be revitalized and modified to put it into daily meso-scale prediction.

ACKNOWLEDGEMENT

This work is supported by the U.S. Army Research Office, Research Triangle Park, North Carolina under Grant DAAG-29-78-G0012.

REFERENCES

1. Abe, M., 1941: Mountain Clouds, their forms and connected air currents, Part II. Bull, Central Met. Observatory of Japan, VII, No. 3, 93-145.

2. Blumen, W. and C. D. McGregory, 1975: Wave drag by three-dimensional mountain lee-waves in non-planar shear flow. Tellus, 28, 287-298.

3. Crapper, G. D., 1962: Waves in the lee of a mountain with elliptical contours, Phil. Trans. Royal Soc., London, 4, 254, 601-623.

4. Davidson, B. and P. K. Rao, 1958: Preliminary report on valley wind studies in Vermont, 1957. College of Engineering, New York University, Final Report, under Contract No. AF 19(604) 1971, 54PP.

5. Davidson, B. and P. K. Rao, 1963: Experimental Studies of the valley-plain wind. Int. J. Air Wat. Poll., 7, 907-923.

6. Endinger, J. G. and M. G. Wurtele, 1972: Interpretation of phenomena observed in California stratus. Mon. Wea. Rev., No. 5 (1972) 389-398.

7. Gjevick, B. and T. Marthinsen, 1978: Three-dimensional lee-wave pattern. Quart. J. R. Met. Soc., 104, No. 442, 947-958.

8. Onishi, G., 1961: The airflow over mountains with constant wind shear, II. Three-dimensional solution. Scientific Report, Tohoku University Ser. 5, Geophys., 12, 169-183.

9. Onishi, G., 1969: Numerical method for three-dimensional mountain waves. J. Met. Soc., Japan, 47, 352-359.

10. Palm, E., 1958: Two-dimensional and three-dimensional mountain waves. Geof. Publc, 20, No. 3, 25PP.

11. Pekelis, E. M., 1966: A numerical solution of three-dimensional non-linear problem of airflow around an obstacle. (In Russian), World Meteorological Center Publication No. 16.

12. Sawyer, J. S., 1962: Gravity waves in the atmosphere as a three-dimensional problem. Quart. J. R. Met. Soc., 88, No. 378, 412-425.

13. Tang, W., 1968: Theoretical Studies of Valley Circulation. Final Report, under Contract No. DAAD-09-67-C-0117. GCA Corporation, Bedford, Mass.

14. Vergeiner, I., 1975: A numerical model of three-dimensional induced gravity wave flow. Riv. Ital. Geofis., 1, 15-31.

15. Vergeiner, I., 1976: Föhn-und Leewellenströmung in einem dreidimensionalen numerischen Modell. Ber. Nat. Med. Ver. Innsbruck, 63, 11-56.

16. Wurtele, M. G., 1957: The three-dimensional lee wave. Beitr. Phys. Atm., 29, 242-252.

THEORETICAL STUDY
OF
THREE-DIMENSIONAL SLOPE
AND
VALLEY WIND SYSTEMS

PART II. PARAMETERIZATION OF THE ATMOSPHERIC SURFACE LAYER AND ACTIVE SOIL LAYER WITH THE PRECIPITATION AND SOIL MOISTURE CONTRIBUTIONS

Wen Tang
University of Lowell
Lowell, Massachusetts 01854

Lev N. Gutman
Tel-Aviv University
Tel-Aviv, Israel

TABLE OF CONTENTS

LIST OF FIGURES

LIST OF TABLES

ABSTRACT

Based upon the contemporary theoretical concept and the incorporation of a model recently developed by Kazakov and Lazriyev (1978), a parameterization of the atmospheric surface layer interacting with active soil layer is made by taking into account of precipitation and soil moisture contributions. A method for predicting surface layer meteorological variables is developed and can be realized as a subroutine in numerical prediction even over non-homogeneous terrain. The development of the proper heat and moisture fluxes boundary conditions based on this study will facilitate the solving of meso-scale and larger scale circulation problems.

I. INTRODUCTION

In order to study meso-scale atmospheric dynamics and boundary layer problems, the equations governing the atmospheric surface layer and the remaining part of the atmosphere, and sometimes an equation of the active soil layer, are usually solved jointly. Previous works that took such an approach are by, for example, Estoque (1961) and Physick (1976) for meso-scale dynamics, and Estoque (1963) and Krishna (1968) for atmospheric boundary layer studies. Because of the complexity of the problems, it has been difficult to obtain the optimum realization of the surface layer model as well as of the main problem, i.e., of the model for the remaining part of the atmosphere.

Gutman (1954) devoted his work to soil temperature calculation where a more convenient approach was applied, in which the surface layer equations are transformed. The effects of the surface layer on the soil layer are formulated, although the appearance of the boundary conditions tend to become more complicated. In the present paper, the advantages of this approach over others is that the surface layer model and the main problem for the layer above can be attacked almost independently. Kazakov and Lazriyev (1978) have recently taken such an approach to parameterize the surface layer in its interaction with the active soil layer on the basis of current theoretical concepts and observational data. In generalizing this later model we have taken into consideration the soil moisture and precipitation contributions based upon the development by Deardorff (1978).

II. THE CASE WHEN THE SURFACE TEMPERATURE AND MOISTURE ARE KNOWN

It can be proved that the constant flux concept remains valid for the surface layer over topographically inhomogeneous terrain under nonstationary conditions as long as the following assumptions can be met:

1. Characteristic time-scale of the processes are greater than a few score minutes, and
2. Characteristic horizontal length scales of the processes are in the order of ten times the thickness of the surface layer (i.e., ∿500 m) or higher.

Under such assumptions the following relationships

$$K_u \frac{\partial u}{\partial z} = C_D V u, \quad K_u \frac{\partial v}{\partial z} = C_D V v \tag{1}$$

$$K_\theta \frac{\partial T}{\partial z} = C_H V (T - T_g), \quad K_\theta \frac{\partial q}{\partial z} = C_H V (q - q_g) \tag{2}$$

$$\left(C_D = C_u^2 , \quad C_H = C_u C_\theta \right)$$

(all notations are explained at the end of this paper)
can be used as boundary conditions for meso-meteorological and planetary boundary problems at z = h, including the problem of mountain-valley circulation when the terrain slope is not exceedingly large. It is understood that T_g, q_g and h in this section are given functions of x, y, and t.

In the paper by Kazakov and Lazriyev (1978) a simple method to calculate C_D and C_H as functions of Ri_B and H,

$$Ri_B = \frac{\lambda h (T_h - T_g)}{V_h^2}, \qquad Ho = \frac{h}{z_o} \tag{3}$$

was suggested. Although V_h, T_h are not known in advance, one can either determine V_h, C_D and C_H by iterations by taking V_h, C_D and C_H from the previous time steps in the actual computation. If one wants to obtain the continuous fields of turbulence at z = h, one can use the formulae,

$$\left.\begin{aligned} (K_i)_h &= \frac{k\sqrt{C_D}V_h h}{\phi_i(\zeta_h)} \quad , \\ \text{and} \quad \left(\frac{\partial K_i}{\partial z}\right)_h &= \frac{(K_i)_h}{h}\left[1 - \zeta_h \frac{d \ln \phi_i(\zeta_h)}{d\zeta_h}\right] \quad , \\ (i = u,\theta) \quad , & \end{aligned}\right\} \tag{4}$$

to determine the coefficients of eddy viscosity and diffusivity and their derivatives as shown in Eq. (4). Empirical functions ϕ_i and f_i are presented in Table 1. The calculation of the distribution of meteorological elements u, v, t and q inside the surface layer can be obtained from the following equations:

$$u = u_h \frac{f_u(\zeta,\zeta_o)}{f_u(\zeta_h,\zeta_o)} \quad , \quad v = v_h \frac{f_u(\zeta,\zeta_o)}{f_u(\zeta_h,\zeta_o)} \tag{5}$$

$$T - T_g = (T_h - T_g) \frac{f_\theta(\zeta,\zeta_o)}{f_\theta(\zeta_h,\zeta_o)} \, , \tag{6}$$

$$q - q_g = (q_h - q_g) \frac{f_\theta(\zeta,\zeta_o)}{f_\theta(\zeta_h,\zeta_o)} \tag{7}$$

in which

$$\zeta = \frac{Z}{h}\zeta_h \, , \quad \zeta_o = \frac{\zeta_h}{H_o}$$

where ζ_h is a function of both Ri_B and H, and ζ_h can be calculated by formulae as indicated in the work by Kazakov and Lazriyev (1978). The heat and moisture fluxes at level h can then be simply expressed, respectively, as

$$H = \rho c_p C_H V_h (T_g - T_h) \tag{8}$$

and

$$E = \rho C_H V_h (q_g - q_h) \tag{9}$$

TABLE 1. Analytical expressions of empirical functions ϕ_i and f_i for various thermal conditions.

$i = u, \theta$	Unstable		Stable	
	Strong	Weak	Strong	Weak
	$\zeta' H \leq \zeta \leq \zeta'$	$\zeta' \leq \zeta \leq o$	$\zeta'' \leq \zeta \leq \zeta'' H$	$o \leq \zeta \leq \zeta''$
$\left[\alpha(o)\right]^{\frac{i-u}{\theta-u}} \phi_i(\zeta)$	$\eta_i(\zeta')(\frac{\zeta'}{\zeta})^{1/3}$	$\eta_i(\zeta)$	$\left(\frac{1}{\zeta''} + \beta_i\right)\zeta$	$1 + \beta_i \zeta$
$\left[\alpha(o)\right]^{\frac{i-u}{\theta-u}} f_i(\zeta,\zeta_o)$	$3\eta_i(\zeta')\left[1-(\frac{\zeta'}{\zeta})^{1/3}\right] + \Phi_i(\zeta') - \Phi_i(\zeta_o)$	$\Phi_i(\zeta) - \Phi_i(\zeta_o)$	$\ln\frac{\zeta''}{\zeta_o} + \frac{\zeta}{\zeta''} - 1 + \beta_i(\zeta-\zeta_o)$	$\ln\frac{\zeta}{\zeta_o} + \beta_i(\zeta-\zeta_o)$

Remarks:

$$\Phi_u(\zeta) = \ln(-\zeta) + 2\,\mathrm{arccot}(\eta_u) - \ln\frac{(1+\eta_u^2)(1+\eta_u)^2}{4\eta_u}$$

$$\Phi_\theta(\zeta) = \ln(-\zeta) - 2\ln\frac{1+\eta_\theta}{\eta_\theta}$$

$$\eta_u(\zeta) = (1-\gamma_u\zeta)^{-1/4} \quad , \quad \eta_\theta(\zeta) = (1-\gamma_\theta\zeta)^{-1/2}$$

III. THE FORMULATION OF THE EQUATIONS FOR THE CASE WHERE THE INITIAL SURFACE TEMPERATURE AND MOISTURE ARE NOT KNOWN

For determining the surface temperature, T_g, and moisture q_g, the problem has to contain the description of heat and moisture exchange in the active layer of soil, and the interaction between the soil and the air. It is essential that these equations are simple enough for constructing the algorithm which must be convenient to apply to the complicated problems of atmospheric dynamics. First let us begin the description of the model with the equation of heat conduction in the soil.

$$\frac{\partial}{\partial t}\theta = \nu \frac{\partial^2 \theta}{\partial z^2} \qquad (z = o) \qquad (10)$$

It is well known that the thermal conductivity of the soil depends mostly upon the soil moisture, and to a lesser extent on temperature, the structure of the soil density. However, the detailed information concerning the soil moisture changes with depth and also other aforementioned properties are not available. Thus it would be appropriate to assume that, for a first approximation, the thermal diffusivity, ν, depends on moisture only at the ground surface level so that we can apply the empirical relationship to calculate the soil diffusivity as shown below:

$$\nu = \frac{0.001 + 0.0004\ Wg^{1/3}}{0.27 + Wg} \quad (Cm^2 sec^{-1}) \qquad (11)$$

which is adopted from Benoit (1976) and Sellers (1975).

In order to solve Equation (10) we regard it as a two point boundary value problem. By assuming both the absence of the heat flow from the deeper layers of soil below and also a constant soil

temperature at a great depth, we may write the lower boundary condition as

$$\theta|_{z=-\infty} = \text{constant} \tag{12}$$

for a given location based on available climatological data. If we assume that the so-called viscous-sublayer is absent, it would be quite natural to acquire continuity at the temperature field at the soil-air interface, i.e.,

$$\theta|_{z=o} = T_g \tag{13}$$

It is noteworthy that the inclusion of the viscous sublayer does not actually complicate matters technically (see Zilitinkevich, 1970). However, no report in open literature has indicated that the inclusion of the sublayer in atmospheric dynamics models has provided better results.

As for the second boundary condition at z = o, we make use of the heat energy balance equation, as usual at the ground surface,

$$G = (1 - \alpha_g)\, S + \varepsilon_g R - \varepsilon_g \sigma T_g^4 - H - LE \quad (\text{at } z = o) \tag{14}$$

where

$$G = \rho_s c_s \nu \frac{\delta\theta}{\delta z}\Big|_{z=o} \tag{15}$$

$$R = \left[\sigma_c + (1 - \sigma_c)\, 0.67\, (1.67 \times 10^3\, q_a)^{0.08}\right] T_a^4 \tag{16}$$

and

$$\alpha_g = 0.31 - 0.17\, W_g/W_k \quad , \quad (W_g < W_k)$$

or (17)

$$\alpha_g = 0.14 \quad , \quad (W_g \geq W_k)$$

The last two relationships are suggested by Staley and Jurica (1972) and Idso et al (1975). For the soil moisture equations we will adapt the force restore method by writing the rate of change of soil moisture in non-dimensional form as shown in the following:

$$\frac{\partial \psi}{\partial t} = \frac{P - E}{\rho_w d_2' W_{max}} \quad , \quad (0 \leq \psi \leq 1) \tag{18}$$

and

$$\frac{\partial \psi_g}{\partial t} = C_1 \frac{P - E}{\rho_w d_1' W_{max}} + C_2 \frac{\psi - \psi_g}{\tau_1} \quad , (0 \leq \psi_g \leq 1) \tag{19}$$

where

$$\psi = \frac{W_2}{W_{max}} \quad , \quad \psi_g = \frac{W_g}{W_{max}} \quad , \tag{20}$$

$$C_1 = \begin{cases} 14 \quad , & (\psi_g \leq 0.15) \\ 14 - 22.5\,(\psi - 0.15), & (0.15 < \psi_g < 0.75) \\ 0.5, & (\psi_g \geq 0.75) \end{cases} \tag{21}$$

$$C_2 = 0.9 \quad , \quad \tau_1 = 6400 \text{ sec} \quad ,$$

$$d_1' = 10 \text{ cm} \quad , \quad d_2' = 50 \text{ cm} \quad .$$

It is seen from Eq. (18) and (19) that the rate of change of moisture content is directly proportional to the difference

between the rate of precipitation and that of evaporation. The inequalities in the brackets indicate that Equations (18) and (19) are valid only when the values of ψ_g and ψ are between o and 1. Beyond these limits the rate change of soil moisture can be negative after reaching the maximum value of W_{max} that soil moisture cannot continuously increase and the extra moisture will be runoff.

In order to eliminate some unknown variables we use the following relationships, based on (6) and (7):

$$T_a - T_g = (T_h - T_g)\ \beta \tag{22}$$

$$q_a - q_g = (q_h - q_g)\ \beta \tag{23}$$

where

$$\beta = f_\theta\ (\zeta_a, \zeta_o)/f_\theta(\zeta_h, \zeta_o)$$

and (24)

$$\zeta_a = \frac{a}{h}\ \zeta_h$$

From an empirical relationship suggested by Deardorff (1978) we present the saturated specific humidity at ground surface in the following form:

$$q_g = \alpha Q_g + (1 - \alpha)\ q_a \tag{25}$$

$$\alpha = \begin{cases} \alpha' & (q_g < Q_g) \\ 1 & (q_g \geq Q_g) \end{cases} \tag{26}$$

where

$$\alpha' = \begin{cases} w_g/w_k, & (w_g < w_k) \\ 1 \quad . & (W_g \geq W_k) \end{cases} \tag{27}$$

$$\left.\begin{aligned} Q(T) &= \frac{3.80}{p} \cdot 10^{7.63\left[\frac{T-273^\circ}{T-31.1^\circ}\right]} \\ Q_g &= Q(T_g), \quad p = 1000 \text{ mb} = \text{const} \end{aligned}\right\} \tag{28}$$

Attention should be paid to the inequalities in (26) and (27). In case q_g in (25) becomes larger than Q_g we should put q_g equal to Q_g. Thus the possibility of condensation of moisture at ground surface is taken into account. We come now to the inequality in (27), which means that after the concentration of soil moisture at ground reaches a certain critical value W_k, less than the W_{max}, the further increase of soil moisture will not change its influence on the air in the surface layer. The pressure in the formula for saturated moisture and humidity in (28) is assumed constant, quite guaranteeing the required accuracy because this formula is used in this paper only for one level, namely, the ground surface, where relative percentage changes of the pressure are small.

Next we shall discuss the question of the formulation of the initial conditions for (10), (18) and (19). In principle it should be possible to get experimental data about values of soil temperature and moisture at different depths of the active soil layer for a certain instant which we may consider to be the initial value. However, at the present such data is practically unavailable for routine calculations. Therefore, we shall assume that after calculations have been made for quite a long interval of time, the

initial conditions becomes less important, because the amount of moisture in the soil is changing continuously. The moisture change will soon begin to vary quickly as time goes on, depending upon the future development of precipitation and some external factors. At the same time the influence of the initial condition of the moisture gradually fades away. In view of the minor role of the initial condition, the appropriate initial condition under the circumstances may simply be assumed as

$$W_g = W_2 = o \text{ when } t = o \tag{29}$$

Considering (10), a parabolic equation, we solve it with the so-called differential equation with no initial condition (See Tikhonov, 1972). Following such an approach, we can solve (10), (18) and (19). It may be worthwhile to point out again here that unless computations have been run for a few hours the results for the beginning time intervals have no true physical meaning and will not agree with the observations in the first few hours.

IV. THE DERIVATION OF THE COMPUTATIONAL FORMULAS.

It is important to construct an algorithm that will be simple enough for practical application. Our problem now is to develop some mathematical expressions similar to (1) and (2), containing parameters which are either known or can be computed so that these expressions can be used as boundary conditions in solving the governing differential equations for the atmospheric dynamics above the ground. First, we want to obtain the expression for heat flux from the soil, G, with known surface temperature, T_g. The main

difficulty is that ν depends upon soil moisture which changes with time. However, the indicated difficulty can be overcome if one can generalize the known expression for the flux

$$\left.\frac{\partial\theta}{\partial z}\right|_{z=o} = \frac{1}{\sqrt{\pi\nu}} \int_{-\infty}^{t} \frac{d\theta_{\zeta=o}(t')}{dt'} \frac{dt'}{\sqrt{t-t'}} \qquad (30)$$

which corresponds to the exact solution for problem (10) with boundary conditions (12) and (13) when ν is constant. When ν is a given function of time, t, (10) may be written in the simpler expressions below, by absorbing ν into ξ through a simple transformation.

$$\frac{\partial\theta}{\partial\xi} = \frac{\partial^2\theta}{\partial z^2} \qquad \left(\xi = \int_o^t \nu(t)dt\right) \qquad (31)$$

The corresponding solution for (31) is then

$$\left.\frac{\partial\theta}{\partial z}\right|_{z=o} = \frac{1}{\sqrt{\pi}} \int_{-\infty}^{\xi} \frac{d\theta_{\zeta=o}(\xi')}{d\xi'} \frac{d\xi'}{\sqrt{\xi-\xi'}} \qquad (32)$$

By changing back ξ into the original notation t, we obtained (33), which is the generalized equation of (30) for the case $\nu = \nu(t)$.

$$\left.\frac{\partial\theta}{\partial z}\right|_{z=o} = \frac{1}{\sqrt{\pi}} \int_{-\infty}^{t} \frac{d\theta_{\zeta=o}(t')}{dt'} \left(\int_{t'}^{t} \nu(t)dt\right)^{-\frac{1}{2}} dt' \qquad (33)$$

For convenience, we introduce time index, j, and time step, Δt, and denote

$$t^j = j.\Delta t \qquad (34)$$

and

$$\phi(t^j) = \phi^j \qquad (\phi = T,\ q,\ \nu,\ \text{etc.}) \tag{35}$$

Furthermore we introduce τ^{j+1},

$$\tau^{j+1} = T^{j+1} - T^j \tag{36}$$

For brevity, we shall drop the time index hereafter if the time step is $j+1$. We should always calculate all variables for the time step $j+1$, as the predicted result for the first time step, in terms of the previous time steps. In order to write (33) in finite difference form, let us replace $\theta_{z=o}(t)$ and $\nu(t)$ by segments of straight lines as shown schematically in Fig. 1. As a result of some elementary transformation we have

$$G = \lambda_g \frac{\partial \theta}{\partial z}\bigg|_{z=o} = M_o \tau_g + \delta, \quad \left(\lambda_g = (c_s \rho_s \nu)_g\right) \tag{37}$$

$$\delta = G^j + N_1 \tau_g^j + N_2 \tau_g^{j-1} + \ldots \tag{38}$$

where

$$\left.\begin{aligned} N_1 &= M_1 - M_o^j \quad , \quad N_2 = M_2 - M_1^j \\ M_o &= \frac{2\lambda_g}{\sqrt{\pi \Delta t}} \frac{1}{\sqrt{\nu}} \\ M_1 &= \frac{2\lambda_g}{\sqrt{\pi \Delta t}} \frac{1}{\sqrt{\nu^j + \nu} + \sqrt{\nu}}, \\ M_2 &= \frac{2\lambda_g}{\sqrt{\pi \Delta t}} \frac{1}{\sqrt{\nu^{j-1} + \nu^j + \nu} - \sqrt{\nu^j + \nu}} \end{aligned}\right\} \tag{39}$$

The expression for δ, generally speaking, is an infinite series, but we truncated the series at the third term for practical purposes. We have performed many numerical calculations, under the assumption

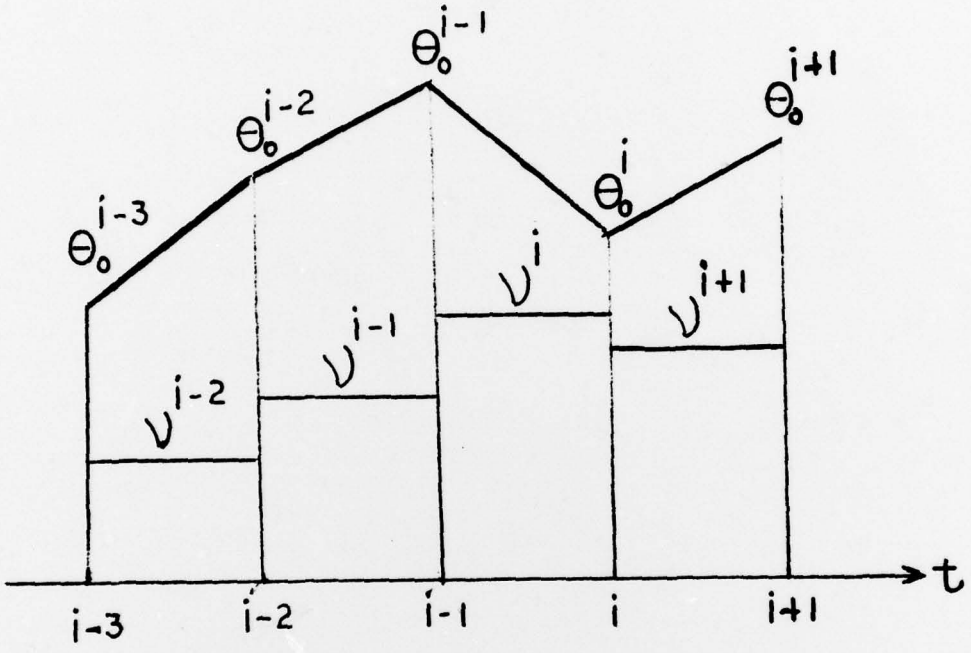

Figure 1. Schematic Diagram of the Variation of Thermal Diffusivity of Soil, ν, and Surface Temperature, θ_o with time t.

that ν = constant, which have shown that the first three terms can provide the accuracy as required if the time increment is not more than 25 - 30 minutes. Thus to use (37), it is necessary to have information of temperature at ground surface for the time steps j - 1 and j in order to calculate the value at time step j + 1.

As to the computation of humidity or moisture at ground surface for the time step j + 1, it can be obtained by solving (18) and (19) by forward time difference method in terms of values at time step j. Having G, one can begin to transform the energy balance equation (14) at ground surface. Prior to the transformation, we want first to linearize the terms contain T_g^4 and T_a^4 and Q_g, by making use of small time step, Δt, in the usual fashion, i.e.,

$$T_g^4 = (T_g^j + \tau_g)^4 = (T_g^j)^4 + 4(T_g^j)^3\tau_g \tag{40}$$

$$T_a^4 = (T_a^j)^4 + 4(T_a^j)^3\tau_a \tag{41}$$

and

$$Q_g = Q_g^j + r_g^j \tau_g$$

$$(r_g^j = \frac{dQ(T)}{dT}) \tag{42}$$

Note that because of the linearity of relationships (22) and (36), the following relationship takes place.

$$\tau_a = (1 - \beta)\,\tau_g + \beta\tau_h \quad . \tag{43}$$

Furthermore, if one solves the system of equations (23) and (25) for unknown variables q_g and q_a, we have then

$$q_a = \frac{\beta\, q_h + \alpha(1 - \beta)\, Q_g}{\beta + \alpha - \alpha\beta} \tag{44}$$

and

$$q_g = \frac{\alpha Q_g + (1 - \alpha)\,\beta q_h}{\alpha + \beta - \alpha\beta} \tag{45}$$

Substituting all necessary parameters H, E, G, T_g^4, T_a^4, and R from (8), (9), (37), (40), (41) and (16), respectively, in addition to the estimated downward short wave radiative flux near the surface, S, into the energy balance equation (14), and solving for the temperature increment τ_g, we have finally, after rearrangement,

$$\tau_g = \frac{1}{A}\,(A_\tau\,\tau_\zeta + A_q\,q_\zeta + A_T) \tag{46}$$

where

$$\left.\begin{aligned} A_\tau &= \rho c_P C_H V_h + 4\,(T_g^{\,j})^3\,\varepsilon_g R\sigma_R \\ A_q &= \frac{L\rho C_H V_h \alpha}{\alpha + \beta - \alpha\beta} \\ A_T &= (1 - \alpha_g)\,S + \varepsilon_g\,\sigma_R\,(T_a^{\,j})^4 + \delta - \varepsilon_g\sigma\,(T_g^{\,j})^4 + \\ &\quad + \rho c_P C_H V_h\,(T_h^{\,j} - T_g^{\,j}) - A_q\,Q_q^{\,j} \end{aligned}\right\} \tag{47}$$

and

$$\begin{aligned} A &= M_o + \rho c_P C_H V_h + A_q\,\varepsilon_g^{\,j} + 4\,(T_g^{\,j})^3\,\sigma\varepsilon_g - \\ &\quad - 4(T_a^{\,j})^3\sigma_R\,\varepsilon_g\,(1 - \beta) \end{aligned} \tag{48}$$

With (46), H, at level A on the top of the surface layer at time step $j^{j'} + 1$, can be obtained from (8) as

$$H = H_\tau \tau_h + H_q q_h + H_T \quad , \tag{49}$$

where

$$\left.\begin{aligned} H_\tau &= \rho c_p C_H V_h A_\tau / A \quad , \\ H_q &= \rho c_p C_H V_h A_q / A \quad , \\ H_T &= (\rho c_p C_H V_\mu A_T / A) + H^j \quad . \end{aligned}\right\} \tag{50}$$

A similar expression can be obtained for E through a somewhat lengthy manipulation, which is shown in the appendix, to yield

$$E = E_\tau \tau_h + E_q q_h + E_T \quad , \tag{51}$$

where

$$\left.\begin{aligned} E_\tau &= f\bar{b} A_\tau / A \quad , \\ E_q &= f(\bar{b} A_q / A - 1) \quad , \\ E_T &= (f\bar{b} A_T / A) + Q^j \quad , \\ f &= \rho C_H V_h \left(\frac{\alpha}{\alpha+\beta-\alpha\beta}\right) \quad , \\ \bar{b} &= \frac{3.80}{p} 10^{7.63} \cdot \left[\frac{4.29 \times 10^3}{10^{1.86 \times 10^3 / T_g}}\right] \quad . \end{aligned}\right\} \tag{52}$$

Except for the coefficients, variables in Equations (49) and (51) are for the time step j+1 at level h and are to be determined. These two equations will serve as boundary conditions for the prognostic equations of diffusion for temperature and moisture in the atmospheric layer above. This set of equations can be solved iteratively

in addition to the momentum equations and their associated boundary conditions, until the solutions converge to a desired accuracy. When q_h and τ_h are determined, the values of q and T at the surface and the intermediate levels in the surface layer can also be easily determined. The proposed more explicit step by step procedure will definitely facilitate the numerical prediction of meteorological variables in meso-meteorology.

V. DISCUSSION

The horizontal wind components, potential temperature, and specific humidity in the surface layer can be simply written in terms of a set of appropriate functions and corresponding specified boundary values, when the time and length scales in consideration are not very small. Their fluxes at the upper boundary can also be expressed in terms of the appropriate boundary values and transfer coefficients which depend upon the Richardson number and the depth of the surface layer. Thus this formulation and parameterization is convenient for studying meso-scale boundary layer problems where the surface layer effect is important. The model can be used to determine the surface temperature and specific humidity at the surface by including the precipitation and soil moisture when the values at the top of the surface layer can be obtained by solving the governing equations in the layer above. Prediction formulae for heat flux are also developed by using finite time difference formulation.

This model and parameterization can be applicable to planetary boundary problems as well as to meso-meteorological problems over mountain terrain (Tang and Peng, 1977). Since mountain-valley circulation results from the interaction between the air in the atmospheric surface layer over the sloping mountain-valley surface and that of higher layers and the ambient atmosphere, the determination of the meteorological variables in the surface layer is essential. The formulation and parameterization developed here will facilitate the numerical experiments of three-dimensional, non-stationary, meso-scale mountain-valley circulation and interaction with the layer scale flow.

Note that the earth's surface, in particular mountain or valley surfaces, is usually covered by forest and vegetation. Based on Deardorff (1978) we made estimations which indicate that the vegetation layer greatly influences the meteorological processes in the boundary layer. Therefore it is our intention to consider the above concept and take this more sophisticated approach to improve the present model of three-dimensional flow over mountain-valley terrain step by step in the near future.

ACKNOWLEDGEMENT

This work is supported by the U. S. Army Research Office, Research Triangle Park, North Carolina under Grant DAAG-29-78-G0012.

NOTATIONS

Arabic

- a anemometer level over the earth surface
- c_s specific heat of soil
- c_p specific heat of air at constant pressure
- C_D drag coefficient
- C_H heat and moisture transfer coefficient
- d_1' soil depth influenced by the diurnal soil moisture cycle
- d_2' soil depth influenced by seasonal moisture variations
- E evaporation rate
- $( )_g$ the subscript g refers to the variable in question at ground surface
- G soil heat flux
- h surface layer height above the ground surface
- H sensible heat flux from the ground (positive when it is upward)
- j time step index
- K_T thermal eddy diffusivity
- K_θ momentum eddy diffusivity
- L latent heat of vaporization
- p mean value of pressure at the ground
- P precipitation rate/mass per unit time and area/specific humidity
- q_a specific humidity at anemometer level
- $q(T)$ saturation specific humidity at temperature T
- Ri_B bulk Richardson number
- R Downward longwave radiative flux
- S influx of shortwave radiation near ground
- t time
- Δt time step interval
- T temperature
- u_* friction velocity
- u,v velocity components in x- and y- axes direction, respectively

Arabic

V	total wind speed
w	volumetric concentration of soil moisture
w_2	vertically averaged value of volumetric moisture concentration in the majority part of d_1' below which the moisture flux is negligible
x,y	horizontal coordinates
z	vertical coordinate/positive upward
z_o	roughness length
W_K	critical or saturated value of w
W_{max}	maximum value of w

Greek

α	degree of soil surface water saturation
α'	fraction
α_g	ground surface albedo
ν	thermal diffusivity of soil
ε_g	ground surface emissivity
θ	soil temperature
θ_g	temperature at $z = o$
ρ	air density
ρ_s	soil density
ρ_w	water density
σ	Stefan-Boltzman constant
σ_c	cloud fraction
λ	buoyancy parameter

Appendix

Derivation of the working formula for moisture at the top of the surface layer, E.

From (8), (25), and (28), E may be written as

$$E = \rho C_H V_h \frac{\alpha}{\alpha+\beta-\alpha\beta} \left[Q_g - q_h \right] \qquad \text{A.1}$$

Because of the non-linear expression of Q_g in T_g, linearization was made from (28), i.e.

$$Q_g = \frac{3.80}{p} 10^{7.63} \left[\frac{Tg - 273^o}{Tg - 31.1^o} \right]$$

$$\simeq \frac{3.80}{p} 10^{7.63} \left(1 - \frac{242.9^o}{Tg} \right)$$

$$= b \cdot \left(\frac{1}{10^{1.86 \times 10^3}} \right)^{\frac{1}{Tg}} \qquad \text{A.2}$$

where $b = \frac{3.80}{p} 10^{7.63}$. Let

$$\varepsilon = \frac{1}{10^{1.86 \times 10^3}} \quad , x = T_g \qquad \text{A.3}$$

Expanding $\varepsilon^{\frac{1}{x}}$ into Taylor's series at $x = x_o$ yields

$$\varepsilon^{\frac{1}{x}} = \varepsilon^{\frac{1}{x_o}} + \frac{\delta}{\delta x} \left(\varepsilon^{\frac{1}{x}} \right)_{xo} (x-xo) + \frac{1}{2!} \frac{\delta^2}{\delta x^2} \left(\varepsilon^{\frac{1}{x}} \right)_{x=x_o} (x-xo)^2 + \ldots \qquad \text{A.4}$$

For $T_g = 300^oK$ and time interval of 20-30 minutes, $(x-x_o)$ will be about 5^oC. in extreme cases. The higher order terms are much smaller than the first order term and can be neglected. Then

$$\varepsilon^{\frac{1}{x}} - \varepsilon^{\frac{1}{x_o}} = -\varepsilon^{\frac{1}{x_o}} \frac{\ln \varepsilon}{x_o^2} \Delta x \qquad \text{A.5}$$

Set $x = T_g^{j+1}$ and $x_o = T_g^j$. Then

$$Q_g^{j+1} - Q^j = b\left[\frac{1}{\varepsilon T_g^{j+1}} - \frac{1}{\varepsilon T_g^j}\right] = b\, b_1 \left(T_g^{j+1} - T_g^j\right) \qquad \text{A.6}$$

where $b_1 = \dfrac{4.29\times10^3}{\left(T_g^j\right)^2}\, 10^{-1.86\times10^3/T_g^j}$

and $b = \dfrac{3.80}{p}\, 10^{7.63}$

Writing in the proper notations defined in this paper and using (46), we have

$$Q_g = \frac{b\, b_1 A_\tau}{A}\, \tau_h + \frac{bb_1 A_q}{A}\, q_h + \left(\frac{bb_1 A_T}{A} + Q_g^j\right) \qquad \text{A.7}$$

Then finally we may write, by using (A.1),

$$E = E_\tau \tau_h + E_q q_h + E_T \qquad \text{A.8}$$

where

$$\left.\begin{aligned} E_\tau &= fbb_1 A_\tau / A \\ E_q &= f(bb_1 A_q / A - 1)\, q_h \\ E_T &= abb_1 A_T / A + Q_g^j \,. \end{aligned}\right\} \qquad \text{A.9}$$

and

$$f = \rho C_H V_h \frac{\alpha}{\alpha+\beta-\alpha\beta}$$

REFERENCES

1. Benoit, R., 1976: A Comprehensive parameterization of the atmospheric boundary layer for general circulation model. Ph.D. thesis, Dept. of Meteorol., McGill Univ., Montreal, Que.

2. Deardorff, J.W., 1978: Efficient prediction of ground surface temperature and moisture, with inclusion of a layer vegetation, Journal of Geophysical Research Vol. 83, No. C4, 1889-1903.

3. Estoque, M.A., 1961: A theoretical investigation of the sea breeze, Quart. J. R. Met. Soc., 87, No. 372, 136-146.

4. Estoque, M.A., 1963: A numerical model of the atmospheric boundary layer, J. Geophys. Res., 68, No. 4, 1103-1113.

5. Gutman, L.N., 1954: A theory for soil temperature calculations, Soviet Research in Geophysics, American Geophysical Union of New York, Volume 1, 1960. Translated from "Transactions of the Geophysics Institute of the Academy of Sciences of the USSR No. 37 (164)."

6. Idso, S.B., Jackson, R.D., Reginato, R.J., Kimball, B.A., and F. S. Nakayama, 1975: The dependence of bare soil albedo on soil water content, J. Appl. Meteorol. 14, 109-113.

7. Kazakov, A.L. and G.L. Lazriyev, 1978: Parameterization of the Atmospheric surface layer and of the active soil layer. Izvestiya, Atm. Oceanic Physics, 14, No. 3, 186-191 (English translation).

8. Krishna, K.A., 1968: A numerical study of the variation of meteorological parameters in the planetary boundary layer, Diurnal variation of winds, Monthly Weather Rev., 96 No. 5, 269-276.

9. Physick, W.L., 1976: A numerical model of the sea breeze phenomenon over a lake or gulf, J. Atmos. Sci., 33, No. 11, 1976, 2107-2135.

10. Sellers, W.A., 1965: Physical Meteorology, University of Chicago Press, Chicago, Ill. 272, pp

11. Staley, D.O. and G.M. Jurica, 1972: Effective atmospheric emissivity under clean skies, J. Appl. Meteorol. 11, 349-356.

12. Tang, W. and L. Peng, 1977: Theoretical study of three-dimensional slope and valley wind systems. Ecological Enterprises, Inc., Bedford, under Contract DAAG 29-76-0007.

13. Tikhonov, A.N. and A.A.Samarsky, 1972: Equations of Mathematical Physics, (in Russian) Nauka.

14. Zilitinkevich, S.S., 1970: Dynamics of the boundary layer of the atmosphere, 1970 (translated into English).